UNIVERSIDADE FEDERAL DE SANTA MARIA
CENTRO DE CIÊNCIAS NATURAIS E EXATAS
PROGRAMA DE PÓS-GRADUAÇÃO EM BIODIVERSIDADE ANIMAL

Micheli Stefanello

DESCRIÇÃO E FILOGENIA DE UM NOVO ESPÉCIME DE CINODONTE PROBAINOGNÁTIO DO TRIÁSSICO SUL-BRASILEIRO

Santa Maria, RS
2018

Micheli Stefanello

DESCRIÇÃO E FILOGENIA DE UM NOVO ESPÉCIME DE CINODONTE PROBAINOGNÁTIO DO TRIÁSSICO SUL-BRASILEIRO

Dissertação apresentada ao Curso de Mestrado do Programa de Pós-Graduação em Biodiversidade Animal, Área de Concentração em Sistemática e Biologia Evolutiva, da Universidade Federal de Santa Maria (UFSM, RS), como requisito parcial para obtenção do grau de **Mestre em Ciências Biológicas – Área Biodiversidade Animal.**

Orientador: Prof. Dr. Sérgio Dias da Silva

Santa Maria, RS
2018

Stefanello, Micheli
DESCRIÇÃO E FILOGENIA DE UM NOVO ESPÉCIME DE CINODONTE PROBAINOGNÁTIO DO TRIÁSSICO SUL-BRASILEIRO / Micheli Stefanello.- 2018.
77 f.; 30 cm

Orientador: Sérgio Dias da Silva
Dissertação (mestrado) - Universidade Federal de Santa Maria, Centro de Ciências Naturais e Exatas, Programa de Pós-Graduação em Biodiversidade Animal, RS, 2018

1. Cinodontes não-mamaliaformes carnívoros 2. Ecteniniidae 3. Triássico Superior 4. Carniano I. Dias da Silva, Sérgio II. Título.

sistema de geração automática de ficha catalográfica da UFSM. dados fornecidos pelo autor(a). sob supervisão da direção da divisão de processos técnicos da biblioteca central. bibliotecária responsável paula schoenfeldt patta CRB 10/1728.

Micheli Stefanello

DESCRIÇÃO E FILOGENIA DE UM NOVO ESPÉCIME DE CINODONTE PROBAINOGNÁTIO DO TRIÁSSICO SUL-BRASILEIRO

Dissertação apresentada ao Curso de Mestrado do Programa de Pós-Graduação em Biodiversidade Animal, Área de Concentração em Sistemática e Biologia Evolutiva, da Universidade Federal de Santa Maria (UFSM, RS), como requisito parcial para obtenção do grau de **Mestre em Ciências Biológicas – Área Biodiversidade Animal.**

Aprovada em 28 de fevereiro de 2018:

Sérgio Dias da Silva, Dr. (UFSM)
(Presidente/Orientador)

Átila Augusto Stock Da-Rosa, Dr. (UFSM)

Téo Veiga de Oliveira, Dr. (UEFS)

Santa Maria, RS
2018

AGRADECIMENTOS

Ao meu orientador, Dr. Sérgio Dias da Silva, pela orientação, por todo o tempo despendido ao longo desse mestrado e por possibilitar meu aprimoramento na área a qual tenho apreço.

Aos colegas do Centro de Apoio à Pesquisa Paleontológica da Quarta Colônia da Universidade Federal de Santa Maria (CAPPA/UFSM) e do Laboratório de Paleobiodiversidade Triássica, dessa mesma instituição, pela convivência e por terem ajudado-me de diferentes formas ao longo do mestrado. Em especial, ao colega Rodrigo Temp Müller, pela coleta do espécime (objeto de estudo dessa dissertação), por toda a ajuda com o TNT e com as figuras, e por auxiliar-me de inúmeras formas. Agradeço também ao Dr. Leonardo Kerber que sempre se dispôs a ajudar-me e por conseguir realizar a tomografia computadorizada do material.

Aos curadores, Dra. Marina Bento Soares e Dr. César Leandro Schultz, da Universidade Federal do Rio Grande do Sul (UFRGS), por permitirem o acesso aos espécimes.

Aos alunos e funcionários do Instituto y Museo de Ciencias Naturales de San Juan, Argentina, pelo carinho e acolhimento. Em especial, ao Dr. Ricardo Martínez, pela autorização no acesso aos espécimes estudados e, principalmente, pela orientação, dedicação e carinho.

Ao Dr. Átila Augusto Stock Da-Rosa (UFSM) e ao Dr. Téo Veiga de Oliveira (UEFS), pela participação como membros da banca examinadora dessa dissertação.

Ao Secretário, Sidnei Cruz, e ao Coordenador, Dr. Sandro Santos, do Programa de Pós-Graduação em Biodiversidade Animal da UFSM, por estarem sempre dispostos a auxiliar-me nos problemas burocráticos e pela oportunidade de desenvolver este estudo.

À Coordenação de Aperfeiçoamento de Pessoal de Nível Superior (CAPES), pela bolsa de estudo concedida.

Por fim, agradeço à toda a minha família e amigos pelo apoio constante. Em especial, agradeço aos meus pais, Delvi T. Stefanello e Elisabeth Garlet Stefanello, por toda a educação, compreensão, incentivo e amor. Às minhas irmãs, Francieli Stefanello, Gisieli Stefanello Rossato e Alessandra Stefanello, pelo apoio incondicional. Ao meu noivo, Luciano Somavilla, por toda compreensão, companheirismo, carinho e amor. À minha amiga, Sheila Cassenote Ferreira, pela amizade, momentos de descontração e apoio emocional nos momentos mais difíceis. Enfim, agradeço a todos que de alguma forma contribuíram ao longo dessa jornada.

RESUMO

DESCRIÇÃO E FILOGENIA DE UM NOVO ESPÉCIME DE CINODONTE PROBAINOGNÁTIO DO TRIÁSSICO SUL-BRASILEIRO

AUTORA: MICHELI STEFANELLO

ORIENTADOR: SÉRGIO DIAS DA SILVA

A presente dissertação tem como objetivo principal apresentar a anatomia craniana de um novo espécime de Ecteniniidae, CAPPA/UFSM 0029, coletado em rochas do Triássico Superior. O novo espécime proveniente do afloramento Janner, interior do município de Agudo, Rio Grande do Sul/Brasil, está incluído na Supersequência Santa Maria, Sequência Candelária (Zona de Associação de *Hyperodapedon* – Carniano). Entre os diversos clados de cinodontes probainognátios registrados a partir dos estratos sul-americanos do Triássico Médio e Superior, o clado Ecteniniidae constitui um dos grupos mais enigmáticos, caracterizando-se pela combinação de caracteres basais e derivados, contudo seu registro ainda é escasso. Até o momento, o clado é representado por três espécies, *Ecteninion lunensis* e *Diegocanis elegans*, táxons argentinos, e por uma única espécie brasileira, *Trucidocynodon riograndensis*. Neste estudo, relatamos um crânio e mandíbula quase completos de um novo e grande espécime de *Trucidocynodon riograndensis*. O novo espécime aumenta a representatividade desse grupo de probainognátios para o Triássico Superior Sul-Brasileiro. As análises filogenéticas recuperaram o espécime CAPPA/UFSM 0029 em uma relação de grupo-irmão com *Trucidocynodon riograndensis*, ambos em uma tricotomia com *Ecteninion lunensis* e *Diegocanis elegans*, formando o clado Ecteniniidae. CAPPA/UFSM 0029 compartilha com o holótipo de *Trucidocynodon riograndensis* (UFRGS PV-1051-T) uma combinação única de caracteres, que permitiu atribuí-lo à espécie *Trucidocynodon riograndensis*: (i) processo extranasal do pré-maxilar grande, mas não contatando o nasal; (ii) forame pterygoparoccipital aberto anteriormente; (iii) abertura posterior do forame pós-temporal limitada pelo tabular e esquamosal; e (iv) abertura dorsal externa da fossa paracanina. CAPPA/UFSM 0029 compreende até o momento o maior ecteniniídeo conhecido, contribuindo assim, para o conhecimento da variação do tamanho corporal dentro do grupo. Além do mais, o novo espécime, juntamente com os demais ecteniniídeos, fornece evidências adicionais de que os cinodontes probainognátios carnívoros desempenharam um papel significativo nos ecossistemas do Triássico Superior e representaram uma radiação endêmica para o sudoeste do Gondwana.

Palavras-chave: Eucynodontia. Ecteniniidae. Cinodontes não-mamaliaformes carnívoros. Triássico Superior. Carniano.

ABSTRACT

DESCRIPTION AND PHYLOGENY OF A NEW SPECIMEN OF PROBAINOGNATHIAN CYNODONT FROM THE TRIASSIC OF SOUTHERN BRAZIL

AUTHOR: MICHELI STEFANELLO

ADVISOR: SÉRGIO DIAS DA SILVA

The present dissertation aims to describe the cranial anatomy of a new specimen of Ecteniniidae, CAPPA/UFSM 0029, collected in Upper Triassic rocks. The new specimen, which comes from the Janner outcrop in the outskirts of the municipality of Agudo, Rio Grande do Sul, Brazil, is included in Santa Maria Supersequence, Candelária Sequence (*Hyperodapedon* Association Zone – Carnian). Among the several clades of probainognathian cynodonts recorded from Middle and Upper Triassic strata in South America, Ecteniniidae is one of the most enigmatic groups, characterized by the combination of basal and derived characters, whose record is still scarce. Until now, the clade comprise three species, *Ecteninion lunensis* and *Diegocanis elegans* from Argentina, and a single Brazilian taxon, *Trucidocynodon riograndensis*. In this study, we report an almost complete skull and lower jaw of a new and large specimen of *Trucidocynodon riograndensis*, which increases the representativeness of this probainognathian clade for the Late Triassic of Southern Brazil. The phylogenetic analysis recovered CAPPA/UFSM 0029 in a sister-group relationship with *Trucidocynodon riograndensis*, both in a trichotomy with *Ecteninion lunensis* and *Diegocanis elegans*, forming the clade Ecteniniidae. CAPPA/UFSM 0029 shares with the holotype UFRGS PV-1051-T a unique combination of features, which allowed its attribution to *Trucidocynodon riograndensis*: (i) extranasal process of the premaxilla large but not contacting the nasal; (ii) pterygoparoccipital foramen anteriorly open; (iii) posterior opening of the post-temporal foramen limited by the tabular and the squamosal; and (iv) external dorsal opening of the paracanine fossa. CAPPA/UFSM 0029 is the largest known ecteniniid specimen so far collected, so it contributes to the knowledge of the variation of the body size within the clade. Moreover, the new specimen, together with other ecteniniids, provides additional evidence that carnivore probainognathian cynodonts played a significant role in the Late Triassic ecosystems and represented an endemic radiation in Southwestern Gondwana.

Key-words: Eucynodontia. Ecteniniidae. Carnivore non-mammaliform cynodonts. Late Triassic. Carnian.

LISTA DE FIGURAS

ARTIGO – Skull anatomy and phylogenetic assessment of a large specimen of Ecteniniidae (Eucynodontia: Probainognathia) from the Upper Triassic of southern Brazil

LISTA DE TABELAS

ARTIGO – Skull anatomy and phylogenetic assessment of a large specimen of Ecteniniidae (Eucynodontia: Probainognathia) from the Upper Triassic of southern Brazil

LISTA DE ABREVIATURAS E SIGLAS

CAPPA/UFSM	Centro de Apoio à Pesquisa Paleontológica da Quarta Colônia
UFRGS	Universidade Federal do Rio Grande do Sul
UFSM	Universidade Federal de Santa Maria

SUMÁRIO

APRESENTAÇÃO

A presente dissertação, estruturada de acordo com as normas do Manual de Dissertações e Teses da UFSM (MDT), integra os requisitos necessários para a obtenção do título de Mestre em Ciências Biológicas – Área Biodiversidade Animal, pelo Programa de Pós-Graduação em Biodiversidade Animal da Universidade Federal de Santa Maria. Ela é composta por uma Introdução, um Artigo e Conclusões.

A Introdução inclui uma breve contextualização do clado Cynodontia, de um de seus grupos menos inclusivos, Probainognathia, com enfoque especial à família Ecteniniidae, seguido da apresentação dos objetivos desta dissertação.

O Artigo tem como foco a descrição da anatomia craniana do espécime CAPPA/UFSM 0029, comparações e hipótese de posicionamento filogenético do espécime. O manuscrito é apresentado de acordo com as normas de formatação exigidas pelo periódico científico Zootaxa, no qual o mesmo foi submetido.

Na seção Conclusões é apresentada uma breve recapitulação dos resultados obtidos ao longo deste estudo em relação aos objetivos propostos para esta dissertação.

1 INTRODUÇÃO

Os cinodontes (Cynodontia OWEN, 1861) compreendem um grande clado de sinápsidos que inclui numerosas espécies, tanto não-mamaliaformes quanto mamaliaformes, estas últimas incluindo Mammalia como clado coronal (HOPSON & KITCHING, 2001; LIU & OLSEN, 2010). Formas não-mamaliaformes estavam entre os componentes mais conspícuos da paleofauna continental de tetrápodes terrestres durante o Triássico, ocorrendo em todos os continentes (ABDALA et al., 2006; 2009; MUSSER et al., 2009; ABDALA & RIBEIRO, 2010; BONAPARTE & MIGALE, 2010). O registro mais antigo de Cynodontia data do Permiano Superior e é representado por *Charassognathus gracilis* e *Abdalodon diastematicus* (BOTHA et al., 2007; KAMMERER, 2016). Durante o Triássico, o grupo tornou-se diversificado e abundante, distribuindo-se por todo o Pangeia (ABDALA et al., 2009; ABDALA & RIBEIRO, 2010). A maioria das formas foi extinta até o final do Triássico, embora uma linhagem, a dos Mammaliformes, passou a se diversificar a partir deste momento. Um segundo grupo que sobreviveu ao final do Triássico, porém acabou por se extinguir durante o início do Cretáceo, foram os Trytilodontidae (WATABE et al., 2007; MUSSER et al., 2009).

Eucynodontia é considerado um clado bastante estável (ROWE, 1988), o qual inclui todos os cinodontes mais derivados que *Thrinaxodon* (KEMP, 1982; HOPSON & BARGHUSEN, 1986; LIU & OLSEN, 2010), ou, em outra definição, o clado menos inclusivo incluindo Mammalia e *Exaeretodon* (HOPSON & KITCHING, 2001). Eucynodontia é composto por dois clados menos inclusivos principais, Cynognathia e Probainognathia (HOPSON & BARGHUSEN, 1986; HOPSON & KITCHING, 2001; ABDALA, 2007). Os cinognátios (Cynognathia) incluem táxons basais de hábitos carnívoros (como por exemplo, o gênero *Cynognathus*), sucessivamente parafiléticos em relação a Traversodontidae, a qual inclui por sua vez formas gonfodontes que agrupam uma associação altamente diversa de formas com hábitos herbívoros e/ou onívoros, apresentando uma dentição transversamente alargada (CROMPTON, 1972; LIU & ABDALA, 2014). Por outro lado, os probainognátios (Probainognathia) reúnem numerosas formas carnívoras, insetívoras, onívoras e herbívoras, com uma grande variabilidade de tamanho e morfologia dentária, possuindo desde dentes pós-caninos setoriais comprimidos labiolingualmente até elementos pós-caninos quadrilaterais/multicuspidados. Em Probainognathia se inclui o clado Mammaliaformes, com um único grupo sobrevivente, os

mamíferos (LUO, 1994; HOPSON & KITCHING, 2001; BONAPARTE et al., 2005; 2012; MARTINELLI & ROUGIER, 2007; LIU & OLSEN, 2010; OLIVEIRA et al., 2010).

Considerado monofilético (BONAPARTE et al., 2003; 2005; ABDALA, 2007; MARTINELLI & ROUGIER, 2007; LIU & OLSEN, 2010; SOARES et al., 2014; MARTINELLI et al., 2016), Probainognathia é definido como o grupo mais inclusivo incluindo *Probainognathus* e excluindo *Exaeretodon* (HOPSON & KITCHING, 2001). Os principais caracteres sinapomórficos apresentados pelo clado são: ausência de forame parietal; ausência de ectopterigoides; borda posterior do palato secundário situada no nível da margem anterior da órbita; crista lambdoide separada do arco zigomático por um entalhe em forma de "V"; ausência de expansão lateral das costelas; e cavidade glenoide sem ou com pouca participação do pró-coracoide (*sensu* HOPSON & KITCHING, 2001).

Probainognathia exibe um registro fóssil abundante na fauna Gonduânica Triássica. Na América do Sul, sobretudo no Brasil e na Argentina, são conhecidas cerca de 20 espécies nas sucessões faunísticas do Triássico Médio e Superior (BONAPARTE, 1966; 1969; 1971; MARTÍNEZ & FORSTER; 1996; MARTÍNEZ et al., 1996; 2013; ABDALA et al., 2002; OLIVEIRA et al., 2010; SOARES et al., 2011; MARTINELLI & SOARES, 2016; MARTINELLI et al., 2016; 2017). Entre os diversos clados de probainognátios registrados a partir dos estratos sul-americanos, Ecteniniidae constitui um dos grupos mais enigmáticos (MARTÍNEZ et al., 2013), caracterizado pela combinação de caracteres plesiomórficos (como por exemplo palato ósseo secundário curto) e características apomórficas (por exemplo, imbricamento dos dentes pós-caninos), representando uma radiação endêmica de cinodontes carnívoros para o sudoeste do Gondwana.

Ecteniniidae aparece como mais derivado que Probainognathidae (*sensu* ROMER, 1973; MARTINELLI et al., 2016) e como grupo-irmão de Prozostrodontia (*sensu* LIU & OLSEN, 2010). Nove sinapomorfias suportam a monofilia de Ecteniniidae: (1) comprimento anteroposterior da região rostral igual ao comprimento da região temporal; (2) perfil sub-retangular da região rostral em vista lateral; (3) comprimento da região temporal quase igual ao comprimento da crista sagital; (4) altura da região rostral maior ou igual à altura da órbita; (5) largura constante da fossa temporal ao longo do seu comprimento; (6) palato ósseo secundário termina antes do último dente pós-canino superior; (7) palato ósseo secundário termina anteriormente à borda anterior da órbita; (8) palatino curto contribui com menos de 1/3 do

comprimento anteroposterior do palato ósseo secundário; (9) ângulo posteroventral do dentário próximo à articulação mandibular (MARTÍNEZ et al., 2013).

Até o momento, o clado Ecteniniidae é representado por três espécies, *Ecteninion lunensis* Martínez et al. 1996 e *Diegocanis elegans* Martínez et al. 2013, táxons argentinos, e por uma única espécie brasileira, *Trucidocynodon riograndensis* Oliveira et al. 2010. No ano de 2012, durante um trabalho de campo em uma localidade fossilífera no interior do município de Agudo, Rio Grande do Sul, foi coletado o material CAPPA/UFSM 0029. Esse afloramento, conhecido como sítio Janner, vem produzindo um conjunto significativo de vertebrados fósseis (LANGER et al., 2007; OLIVEIRA et al., 2007; 2010; CABREIRA et al., 2011; LIPARINI et al., 2013; MÜLLER et al., 2016; 2017) e está incluído na Sequência Candelária da Supersequência Santa Maria, de idade Carniana, com base na presença do rincossauro *Hyperodapedon* (LANGER et al., 2007; 2018; HORN et al., 2014). As análises filogenéticas recuperaram o espécime CAPPA/UFSM 0029 em uma relação de grupo-irmão com *T. riograndensis*, e ambos em uma tricotomia com *E. lunensis* e *D. elegans* dentro do clado Ecteniniidae. Este novo espécime de *T. riograndensis* é foco principal do estudo desta dissertação de Mestrado.

2 OBJETIVOS

Esta dissertação de Mestrado tem por objetivo geral tornar conhecida a anatomia craniana do espécime CAPPA/UFSM 0029 e realizar sua identificação taxonômica no menor nível possível.

2.1 Objetivos específicos

(i) Descrever, através da metodologia usual em paleontologia de vertebrados, detalhes da anatomia craniana de CAPPA/UFSM 0029.

(ii) Através de análise filogenética, testar a relação de proximidade entre o material CAPPA/UFSM 0029 e *Trucidocynodon riograndensis* (UFRGS PV-1051-T).

(iii) Ainda através de análise filogenética, buscar novos caracteres cranianos em CAPPA/UFSM 0029 que contribuam na resolução da politomia entre os membros da Família Ecteniniidae.

3 ARTIGO

Skull anatomy and phylogenetic assessment of a large specimen of Ecteniniidae (Eucynodontia: Probainognathia) from the Upper Triassic of southern Brazil

MICHELI STEFANELLO[1,4], RODRIGO TEMP MÜLLER[1,2], LEONARDO KERBER[2], RICARDO N. MARTÍNEZ[3] & SÉRGIO DIAS-DA-SILVA[2]

[1]*Programa de Pós-Graduação em Biodiversidade Animal, Universidade Federal de Santa Maria, 97105-120 Santa Maria, RS, Brazil. E-mail: michelistefanello@hotmail.com, rodrigotmuller@hotmail.com*

[2]*Centro de Apoio à Pesquisa Paleontológica da Quarta Colônia, Universidade Federal de Santa Maria, Rua Maximiliano Vizzotto, 598, 97230-000 São João do Polêsine, RS, Brazil. E-mail: leonardokerber@gmail.com, paleosp@gmail.com*

[3]*Instituto y Museo de Ciencias Naturales, Universidad Nacional de San Juan, Av. España, 400 (norte), 5400 San Juan, Argentina. E-mail: martinez@unsj.edu.ar*

[4]*Corresponding author*

Abstract

Ecteniniidae comprises an endemic radiation of carnivore probainognathian cynodonts from the Late Triassic of South America. Three taxa have been included in this clade: *Ecteninion lunensis* Martínez *et al*., 1996 and *Diegocanis elegans* Martínez *et al*., 2013 from Argentina, and *Trucidocynodon riograndensis* Oliveira *et* al., 2010 from Brazil. Herein, a new specimen (skull and mandible) assigned to *T. riograndensis* from the Carnian of the Candelária Sequence is described. A phylogenetic analysis recovered the new specimen as the sister taxon of holotype of *T. riograndensis,* and both in a trichotomy with *E. lunensis* and *D. elegans,* all supporting the monophyly of Ecteniniidae. The new specimen of *T. riograndensis* is almost 20% larger than its holotype. It also represents one of the largest specimen of carnivore therapsid from the Late Triassic known to date. The new specimen, together with the holotype of *T. riograndensis*, provides additional evidence that large carnivorous probainognathians played a significant role in Late Triassic ecosystems from southern Brazil.

Keywords: Candelária Sequence. Carnian. Late Triassic. Janner outcrop. Probainognathians. Phylogeny. South America.

Introduction

Probainognathia (sensu Hopson & Kitching 2001; Liu & Olsen 2010) is a heterogeneous group of primarily carnivorous species included in Eucynodontia (Cynognathia + Probainognathia; Hopson & Kitching 2001; Liu & Olsen 2010). The oldest probainognathians are from the early Middle Triassic, and today the group is represented exclusively by the crown group Mammalia. Triassic probainognathians comprise a large variety of body sizes and dental morphologies that vary from sectorial to quadrilateral/multicuspidate postcanine teeth, suggesting distinctive

feeding ecologies (e.g., Liu & Olsen 2010; Abdala & Ribeiro 2010; Bonaparte & Migale 2015). Triassic strata from South America have yielded a large number of non-mammaliaform eucynodonts, which are fundamental to the comprehension of the evolution of this group, as well as to the understanding of the origin of Mammaliaformes (e.g., Bonaparte & Migale 2015; Martinelli & Soares 2016). The herbivorous/omnivorous forms of the clade Gomphodontia are comparatively more abundant in number of specimens than the clade Probainognathia in Carnian strata, represented by several taxa of Traversodontidae (e.g., Abdala *et al*. 2002; Liu *et al*. 2008; Liparini *et al*. 2013). Some taxa of non-mammaliaform probainognathians with strictly carnivorous dentition are well represented in Upper Triassic strata from Brazil and Argentina, such as the chiniquodontids and ecteniniids (Martínez & Forster 1996; Martínez *et al*. 1996; 2013; Oliveira *et al*. 2010). Particularly this latter family comprise one of the most enigmatic group, which is characterized by a combination of basal and derived features (Martínez *et al*. 2013). It is noteworthy that they may represent an endemic radiation of carnivorous cynodonts from western Gondwana.

In the late 1980's, during an expedition aiming to recover early dinosaurs in the northwestern of Argentina, a new species of carnivorous eucynodont was found in the Ischigualasto Formation. The taxon was named later as *Ecteninion lunensis* Martínez *et al*., 1996 and it was recovered as one of the most basal taxa within Eucynodontia, forming a trichotomy with *Probainognathus jenseni* Romer, 1970 and more derived forms (Martínez *et al*. 1996). After that, in 2010, Oliveira and colleagues described a large carnivorous probainognathian from the Late Triassic of Southern Brazil – *Trucidocynodon riograndensis* Oliveira *et al*., 2010, which was placed as the sister-taxon of the smaller Argentinean *E. lunensis* (Oliveira *et al*. 2010). Later, *Diegocanis elegans* Martínez *et al*., 2013, an additional species of a relatively small carnivorous form, was described from the Ischigualasto Formation. The taxon was placed in a trichotomy

with the Argentinean *E. lunensis* and the Brazilian *T. riograndensis* (Martínez *et al*. 2013). Based on these results, Martínez *et al*. (2013) named this group as Ecteniniidae, which is one of the most basal clades of probainognathians.

Despite the innumerous new discoveries from Upper Triassic strata in South America, the fossil record of ecteniniids is still scarce. In the present contribution, we report an almost complete skull and mandible of a new and large specimen referred to *T. riograndensis*, from the Upper Triassic of the Santa Maria Supersequence, Southern Brazil. This specimen comprises the largest known ecteniniid collected so far. In addition, we also provide a cladistic analysis in order to test its relationships and its potential implications for the phylogeny of the group.

Institutional abbreviations: CAPPA/UFSM, Centro de Apoio à Pesquisa Paleontológica da Quarta Colônia da Universidade Federal de Santa Maria, São João do Polêsine, Rio Grande do Sul, Brazil; **GPIT**, Institut und Museum für Geologie und Paläontologie der Universität Tübingen, Germany; **MCP**, Museu de Ciências e Tecnologia da Pontifícia Universidade Católica do Rio Grande do Sul, Porto Alegre, Brazil; **PVSJ**, Instituto y Museo de Ciencias Naturales, San Juan, Argentina; **UFRGS PV-T**, Universidade Federal do Rio Grande do Sul, Paleontologia de Vertebrados, Porto Alegre, Brazil.

Geological Setting

Upper Triassic strata from the State of Rio Grande do Sul, especially those from the Santa Maria Supersequence (Zerfass *et al*. 2003) include an abundant and diverse fossil record of tetrapods (e.g., Langer *et al*. 2007; Abdala & Ribeiro 2010; Martinelli & Soares 2016). The Santa Maria Supersequence is divided into four depositional sequences (with their respective tetrapod Assemblage Zones – AZ), from bottom to top, as follows: Pinheiros-Chiniquá (*Dinodontosaurus*

AZ, Ladinian/early Carnian), Santa Cruz (*Santacruzodon* AZ, early Carnian), Candelária (*Hyperodapedon* AZ, late Carnian; *Riograndia* AZ, Norian), and Mata (Raethian) sequences (Zerfass *et al*. 2003; Horn *et al*. 2014; see also Schultz *et al*. 2000; Soares *et al*. 2011).

The specimen CAPPA/UFSM 0029 comes from the fossiliferous locality known as Janner outcrop, which belongs to the Candelária Sequence (Fig. 1). This site, located about 2 km from the urban area of the municipality of Agudo, shows a considerable fossil diversity (e.g., Oliveira *et al*. 2010; Cabreira *et al*. 2011; Liparini *et al*. 2013) and is regarded as belonging to the *Hyperodapedon* AZ. Lithologically, the Janner outcrop comprises massive red beds, including siltstones and very thin-grained sandstones. This locality incorporates mud inclusions and sporadic rhythmic intervals of various grain sizes. The red beds are subdivided in a non-fossiliferous portion at the base of the exposed section, a middle unit, greatly fossiliferous, and a large layer of sandstone above the fossiliferous level, also devoid of fossils. Based on sedimentology and in the presence of coprolites and putative rhizoliths, the strata are interpreted as accumulated in a distal floodplain paleoenvironment (Pretto *et al*. 2015). According to Zerfass *et al*. (2003), the predominant lithofacies in this unit are non-laminated to finely laminated reddish mudstones with some sandy inclusions. Fonseca (1999) also interpreted these deposits as a fluvial system with channels that ranged from stable to sinuous, where the siltstones represent floodplains and the sandy lenses characterize fluvial channels.

The Janner site has produced a significant suite of fossil tetrapods: the ecteniniid *Trucidocynodon riograndensis* (Oliveira *et al*. 2010), the traversodontid *Exaeretodon riograndensis* Abdala *et al*., 2002 (Oliveira *et al*. 2007; Liparini *et al*. 2013), an briefly mentioned ictidosaur (Martinelli *et al*. 2016a), the rhynchosaur *Hyperodapedon* Huxley,1859 (Langer *et al*. 2007), the early sauropodomorph dinosaur *Pampadromaeus barberenai* Cabreira *et*

al., 2011 (Müller *et al*. 2016; 2017), and indeterminate dinosauriforms (Müller *et al*. 2014; Pretto *et al*. 2015).

It is important to point out the remarkable abundance of specimens of the traversodontid *E. riograndensis* (dozens deposited at the collection of CAPPA/UFSM, for instance) from the middle section of Janner site. This taxon greatly exceeds the record of the rhynchosaur *Hyperodapedon* (Oliveira & Schultz 2007; Liparini *et al*. 2013; Müller *et al*. 2015; Pretto *et al*. 2015). Due to this proportion, the Janner site was chronologically placed in the upper portion of the *Hyperodapedon* AZ (Langer *et al*. 2007), which allows the correlation of this outcrop with the fossil fauna from the Ischigualasto Formation from northwestern Argentina. This biostratigraphic correlation suggests a Late Carnian age to the Janner outcrop, based upon the radioisotopic dating accomplished in the Argentinean formation (Martínez *et al*. 2011; Langer *et al*. 2018).

Material and methods

Collection, anatomy and comparison. The specimen CAPPA/UFSM 0029 was collected during a fieldwork in 2012, in the outskirts of the municipality of Agudo, State of Rio Grande do Sul, Southern Brazil. Anatomical nomenclature follows previous descriptions of cynodonts (Martínez *et al*. 1996; 2013; Hillenius 2000; Sidor 2003; Oliveira *et al*. 2010). Comparisons with other basal probainognathians were carried out with first-hand examination of specimens by MS in Brazilian and Argentinean collections (*Trucidocynodon riograndensis*: holotype UFRGS PV-1051-T; *Ecteninion lunensis*: holotype PVSJ 422 plus the specimens PVSJ 481, PVSJ 692, PVSJ 693; *Diegocanis elegans*: holotype PVSJ 881; *Chiniquodon sanjuanensis* Martínez & Forster 1996: holotype PVSJ 411) and descriptions of other non-mammaliaform cynodonts from literature. Measurements of the structures present in CAPPA/UFSM 0029 were performed following those made by Oliveira *et al*. (2010) for the holotype of *T. riograndensis* (Table 1).

Computed tomography. In order to visualize the internal structures and generate a 3D model, the specimen was scanned in a medical clinic (Dix – Diagnóstico por Imagem do Hospital de Caridade) in the municipality of Santa Maria, Rio Grande do Sul. A Philips Brilliance 16-Slice CT Scanner, with voltage of 140 kV and amperage of 275 mA was used, in which 589 slices were generated with slice thickness of 0.8 mm and interslice of 0.4 mm. The image resolution is 512 x 512 pixels. The raw scan data were exported from the scanner computer in DICOM format.

Phylogenetic analysis. CAPPA/UFSM 0029 was included in the dataset of Martinelli *et al*. (2016b), in order to test its phylogenetic affinities. In addition, we also incorporated *Trucidocynodon riograndensis* Oliveira *et al*., 2010 and *Diegocanis elegans* Martínez *et al*., 2013 in the dataset. The scores for both taxa follow those provided by Martínez *et al*. (2013) and were checked by first hand observation of the specimens UFRGS PV-1051-T (*T. riograndensis*) and PVSJ 881 (*D. elegans*). Three cranial characters (4, 10, and 19) proposed by Martínez *et al*. (2013) also were included in the dataset. These characters were respectively renumbered here as 146, 147, and 148. The character number three was modified following the new definition and states proposed by Martínez *et al*. (2013). After these modifications, the dataset included 148 characters and 38 operational taxonomic units (OTUs) (see Supporting Information).

The phylogenetic analysis was conducted in the software TNT v1.1 (Goloboff *et al*. 2008). All characters received the same weight and were treated as unordered. *Procynosuchus delaharpeae* Broom, 1937 was used to root the most parsimonious cladograms (MPCs), which were recovered via ‘Traditional search’ (random addition sequence + tree bisection reconnection) with 1000 replicates of Wagner trees (with random seed = 1), tree bisection reconnection and

branch swapping (holding 20 trees save per replicate). Decay indices (Bremer support values), as well as bootstrap values (1000 replicates), were also obtained with TNT v1.1.

Systematic Paleontology

Therapsida Broom, 1905

Cynodontia Owen, 1861

Eucynodontia Kemp, 1982

Probainognathia Hopson, 1990

Ecteniniidae Martínez, Fernandez & Alcober, 2013

***Trucidocynodon riograndensis* Oliveira, Soares & Schultz, 2010** (Figs. 2-8; Table 1)

Holotype: UFRGS PV-1051-T, almost complete skeleton (Oliveira *et al*. 2010).

Paratypes: UFRGS PV-1053-T, right scapular girdle and forelimb; UFRGS PV-1069-T, five vertebrae and some fragmentary ribs; UFRGS PV-1070-T, a right tibia; UFRGS PV-1071-T, right ulna (Oliveira *et al*. 2010).

Diagnosis: See Oliveira *et al*. 2010.

Referred specimen: CAPPA/UFSM 0029, a complete skull including articulated lower jaw, with about 225 mm in total length.

Locality and horizon: CAPPA/UFSM 0029 comes from the Janner outcrop, municipality of Agudo, State of Rio Grande do Sul, Brazil, which is included in the lower portion of the Candelária Sequence (Horn *et al*. 2014), *Hyperodapedon* AZ, Santa Maria Supersequence (Zerfass *et al*. 2003).

Taphonomic remarks. The almost complete skull and lower jaw of CAPPA/UFSM 0029 suffered a degree of dorsolateral compression (Figs. 2-8). The sutures of the preorbital region and

skull roof are well defined, being possible to identify all bone contacts. In other regions, however, the sutural limits are neither completely visible nor preserved. The anterior region of the secondary palate is covered by incrustation that was irremovable during preparation; the posterior region (including the posterior portion of the horizontal lamina of the maxilla and the palatine) is not preserved. Sutural contacts of the basicranial region and of the braincase are mostly unclear. Accordingly, we only provide an overall description of both braincase and basicranium. Although presenting taphonomic modifications, the specimen is very less laterally flattened than the holotype of *T. riograndensis* (UFRGS PV-1051-T), allowing a more reliable interpretation of the general shape of the skull.

Description and comparison

Premaxilla. CAPPA/UFSM 0029 preserves both premaxillae (Figs. 2-5). The main body of this element is proportionally larger than in traversodontid cynodonts (e.g., *Exaeretodon riograndensis*), with proportions resembling those of other ecteniniids. The internarial process of CAPPA/UFSM 0029 is tall, but does not reach the nasals (Figs. 2-5). In lateral view, it is dorsally directed in its ventral half, whereas the dorsal part is dorsoposteriorly directed, similarly to *Ecteninion lunensis*. This structure is sigmoid in lateral view in *Diegocanis elegans* (although this could be taphonomic), and in the holotype of *Trucidocynodon riograndensis* it is missing (Oliveira *et al*. 2010). The posterolateral ascending process is long and reaches the dorsal level of the external nares, but does not contact the nasal, similar to the condition of holotype UFRGS PV-1051-T and *Chiniquodon sanjuanensis* (PVSJ 411). In contrast, it is short in *E. lunensis* and *D. elegans* (Martínez *et al*. 2013). The posteroventral border of the premaxilla contacts the anteroventral margin of the maxilla at the level of the fourth upper incisor, as in the holotype of *T. riograndensis*, *E. lunensis*, and *D. elegans* (Martínez *et al*. 1996; 2013; Oliveira *et al*. 2010). In

dorsal view, the posterolateral ascending process of the premaxilla of CAPPA/UFSM 0029 ends at the anterior border of the paracanine fossa, which is opened dorsally (Figs. 2-5, 8).

Septomaxilla. Both septomaxillae are almost complete, and only the left portion of the intranarial process (= medial lamina) (see Hillenius 2000; Sidor 2003) is missing (Figs. 2-5). The right intranarial process covers the dorsal surface of the premaxilla in CAPPA/UFSM 0029. It is ventrally convex, dorsally concave, and extends towards the midline, separated from the narial floor, as in *D. elegans*. The facial (=ascending) process appears to be proportionally less developed than in *E. lunensis* and *D. elegans*. The dorsal portion of the facial process runs posterodorsally, contacts the posterolateral ascending process of the premaxilla, and delimitates the posterolateral border of the external nares. The opening of the septomaxillary foramen is uncertain.

Maxilla. Both elements are completely preserved (Figs. 2-5). They are subrectangular in lateral view and dorsoventrally deep, a condition found in other ecteniniids. The maxilla occupies almost entirely the lateral surface of the preorbital region (Oliveira *et al*. 2010). As in other eucynodonts, for example *Lumkuia fuzzi* Hopson & Kitching 2001 and *Chiniquodon sanjuanensis*, the maxilla reaches its greatest height at the level of the canine root (Martínez *et al*. 2013). In addition, the dorsal margin of the maxilla is anteroposteriorly shorter in comparison to the ventral margin (Fig. 4), as in *E. lunensis* and in the holotype of *T. riograndensis*, whereas in *D. elegans* this feature is less pronounced. As in other ecteniniids, CAPPA/UFSM 0029 presents two anteroposteriorly aligned infraorbital foramina in the middle region of the maxilla, however in *E. lunensis* and *D. elegans* a third infraorbital foramen is opens laterally at the point where lacrimal, jugal and maxilla contact (Martínez *et al*. 1996; 2013). The posterior portion of the maxilla contacts the jugal posteroventrally, forming the anterior root of the zygomatic arch, the lacrimal posterodorsally, and the nasal margin dorsally (Figs. 2-5). The anterodorsal margin of

the maxilla runs along the nasal and meets the external dorsal opening of the paracanine fossa at the level of the upper canine root. Comparison of the two sides demonstrates that the dorsal opening of the paracanine fossae are slightly deformed. This structure is better preserved on the left side. The right edges of the paracanine fossa measures 6 mm anteroposteriorly and 13 mm dorsoventrally (Fig. 2). Conversely, the left paracanine fossa measures 6 mm anteroposteriorly and 8 mm dorsoventrally (Fig. 3). In contrast to *D. elegans*, in CAPPA/UFSM 0029, UFRGS PV-1051-T, and *E. lunensis* the paracanine fossae are open dorsally (Figs. 4, 8), which allows the tips of the lower canines to protrude through the roof of the snout (Martínez *et al*. 2013).

Nasals. CAPPA/UFSM 0029 preserves both nasals (Figs. 2-4). They comprise approximately 44% of the total length of the skull. Medially, the nasals contact each other in a straight suture. On the anterior half of the nasal, there is a small elevation (anteroposterior convexity) close to the upper premaxillary border. In the holotype of *T. riograndensis* and *E. lunensis*, this region is relatively flat in comparison with its remaining dorsal surface. In *D. elegans*, the entire dorsal profile of the nasal is flat in lateral view. It is plausible that this dorsal convexity in CAPPA/UFSM 0029 is an artifact of preservation, because this region is expanded by diagenesis (Fig. 4). As in other eucynodonts (e.g., holotype of *T. riograndensis, Probainognathus, Chiniquodon* von Huene, 1936), in dorsal view the nasal is curved on the level of the postcanine constriction, whereas in *D. elegans* it gently tapers from the anterior end to the level of the postcanine constriction (Martínez *et al*. 2013). Laterally, the nasal contacts the maxilla (Figs. 2-5). In addition, it expands posterolaterally close to the level of the anterior border of the orbit, so that its posteromedial border contacts the anterior margin of the frontal. Its posterolateral border contacts the anteromedial margin of the prefrontal and the anteromedial margin of the lacrimal. In *D. elegans* the nasal slightly contacts the prefrontal, in contrast to the

condition in CAPPA/UFSM 0029, UFRGS PV-1051-T, and *E. lunensis*, where the contact between these bones is extensive.

Lacrimal. Both elements are practically complete, lacking just a small fragment of the posteroventral end of the right element (Figs. 2-4). As in the other ecteniniids, the lacrimal is anteroposteriorly short, in contrast to *Chiniquodon theotonicus* von Huene, 1936 (GPIT 1050), in which the lacrimal is anteriorly developed, with a triangular shape in lateral view. The anterior lacrimal margin is rounded, forming the anterior and ventral orbital rim. Posterodorsally, the lacrimal contacts the prefrontal and the anteroventral portion of the jugal (Figs. 2-4). The anterodorsal margin of the lacrimal contacts the nasal, whereas its anteroventral portion contacts the maxilla. In CAPPA/UFSM 0029, as in the holotype of *T. riograndensis*, the lacrimal is reduced, because it does not present a posteriorly directed ventral process that forms a pronounced ridge in the orbital margin, a condition found in *D. elegans, E. lunensis* and ictidosaurs (e.g., *Riograndia guaibensis* Bonaparte *et al*. 2001) (Martínez *et al*. 2013). The lacrimal of *D. elegans* is taller than that in other ecteniniids. Thus, this element possibly possesses a large dorsolateral contact with the nasal and a significant participation in the orbital margin.

Prefrontal. Both elements are completely preserved in CAPPA/UFSM 0029, they are rectangular and posteromedially expanded, where they contact the frontals (Figs. 2-4). In dorsal view, the prefrontals are smaller than those from traversodontids (Fig. 4) (e.g., *Exaeretodon riograndensis*, MCP 1522 PV), in which this bone is wide and quadrangular bone (Abdala *et al*. 2002). Conversely, in *D. elegans* and *E. lunensis* the prefrontals are narrower than CAPPA/UFSM 0029 and UFRGS PV-1051-T and do not possess a posteromedial expansion. The prefrontal forms most of the dorsal border of the orbital rim, but does not participate in the medial orbital wall, a condition similar to that found in other ecteniniids as well as in

chiniquodontids (Oliveira *et al*. 2010; Martínez *et al*. 2013). Anteromedially, the prefrontal contacts the posterolateral portion of the nasal and anterolaterally the dorsal margin of the lacrimal, as in the holotype of *T. riograndensis* and *E. lunensis*, but differently from *D. elegans* in which the bone is more anteriorly expanded forming a tiny anteromedial contact with the nasal and the lacrimal (Martínez *et al*. 2013). Medially, it contacts the lateral border of the frontal and, posteriorly, the anterodorsal margin of the postorbital.

Frontal. Both elements are complete and placed in the central portion of the skull roof (Fig. 4). Together, they have shape of lozenge in dorsal view, with a posteriorly projected wedged portion. The frontals articulate against each other, forming a small midline crest that tapers posteriorly, contacting the parietals (Fig. 4). In UFRGS PV-1051-T and *E. lunensis*, the frontals form a midline, flat crest, and in *D. elegans* the suture between frontals is not visible due to poor preservation. The anteroposterior length of the frontals is larger than the transverse width. In CAPPA/UFSM 0029, the frontals have a long posterolateral contact with the postorbitals and a comparatively shorter anterolateral contact with the prefrontal bones (Fig. 4). They also contact the nasals anteriorly and the parietals posterolaterally. In dorsal view, the frontal has two depressions in the anterolateral region (Fig. 4), which could be an indication of a circular foramen as this feature is present on the posterolateral portion in *E. lunensis* (Martínez *et al*. 1996). The frontals of CAPPA/UFSM 0029 do not contact the orbital margin, as in most non-mammaliaform cynodonts (e.g., ecteniniids, *Probainognathus jenseni*, *Lumkuia fuzzi*, and *Exaeretodon riograndensis*). The sutures in the orbital wall cannot be observed, since the internal orbital region is damaged. However, inside the orbit, the frontals of the holotype of *T. riograndensis, E. lunensis,* and *D. elegans* extend ventrally to form part of inner orbital wall, contacting the lacrimal anteriorly, the prefrontal laterodorsally, and the palatine ventrally (Martínez *et al*. 1996; 2013).

Parietal. The parietals of CAPPA/UFSM 0029 are elongate and fused to each other (Figs. 2-4). They comprise approximately 37% of the total skull length in dorsal view and form a tall sagittal crest that arises immediately behind of the level of the posterior orbital margin and extends posteriorly to reach the anterior most portion of the occipital (lambdoidal) crest. Anteriorly, the parietals contact the posteromedial portion of the frontals and postorbitals (Fig. 4). Posteriorly, the parietal contacts the interparietal, which contributes to the posterior portion of the sagittal crest and posteroventrally contacts the squamosal, but there is no clear sign of sutures between these bones. Thus, it is not possible to observe if the squamosal of CAPPA/UFSM 0029 contributes in the formation of the sagittal crest or participates only of the lateral portion of the occipital crest. In *T. riograndensis* (UFRGS PV-1051-T) the squamosal contributes only to the lateral portion of the occipital crest. In contrast, in *E. lunensis* and *Probainognathus* the squamosal contributes to the posterolateral portion of the sagittal crest and posterior portion of the occipital crest, more extensively developed in the latter taxon (Martínez *et al*. 1996). The pineal foramen is absent, as in other probainognathians (Hopson & Kitching 2001; Liu & Olsen 2010).

Postorbital. CAPPA/UFSM 0029 preserves both postorbitals (Figs. 2-4). Dorsally they participate in a small portion of the skull roof, and their sutural contacts are clear. The postorbital bears a posterior process with a semicircular shape, which extends posteriorly towards the skull midline. The posterior process broadly overlaps the posterolateral portion of the frontal and the anteromedial margin of the parietal. Anteriorly, the postorbital also contacts the posterior border of the prefrontal. The postorbital bar forms both posterodorsal and posterior orbital margin. It is thin and subcircular in cross-section, as in the holotype of *T. riograndensis*, *E. lunensis*, and *Chiniquodon sanjuanensis* (Martínez & Forster 1996; Martínez *et al*. 1996; Oliveira *et al*. 2010). In *D. elegans*, this condition is unknown because both the left postorbital and posterior portion of

the right one are not preserved. The postorbital bar of CAPPA/UFSM 0029 contributes a descending process, which anteriorly overlaps the ascending process of the jugal (Fig. 3), a condition shared with the holotype of *T. riograndensis* and *E. lunensis* (PVSJ 481). On the other hand, the holotype of *E. lunensis* (PVSJ 422) does not preserve this region. According to Oliveira *et al*. (2010), *T. riograndensis* (UFRGS PV-1051-T) presents a possible autapomorphic feature in the postorbital: it overlaps the jugal in the ventral margin of the orbit. However, this feature is not an autapomorphy of holotype UFRGS PV-1051-T but, instead, a condition shared with *E. lunensis* (PVSJ 481). In *D. elegans* this feature is unknown.

Jugal. Both sides of the specimen partially preserve this bone (Figs. 2-3). A small anterior portion that contacts the lacrimal anterodorsally and the maxilla anteriorly is displaced from the right element. In addition, both posterior portions of the zygomatic arch are fractured, and the right arch is better preserved than the left one, which is broken on its posterior end. The jugal largely contributes to the zygomatic arch, but due to bad preservation the posterior contact of the jugal and squamosal is uncertain. Compared to other non-mammaliaform cynodonts, the zygomatic arch of CAPPA/UFSM 0029 is narrow and slender, as in UFRGS PV-1051-T and in the preserved anterior portions of the jugal of *D. elegans* and *E. lunensis* (Martínez *et al*. 1996; 2013; Oliveira *et al*. 2010). On the other hand, the zygomatic arch of chiniquodontids, *Probainognathus jenseni*, and other cynognathians (e.g., *Exaeretodon riograndensis*) is more robust. The jugal forms approximately 50% of the posteroventral orbital rim (Fig. 2). Dorsally the lateral portion of the postorbital, CAPPA/UFSM 0029 and *T. riograndensis* (UFRGS PV-1051-T) present a short jugal/lacrimal contact, in contrast to the condition in *D. elegans* and *E. lunensis* (see Martínez *et al*. 1996; 2013). In the posterior portion of the orbital rim, the ascending process of the jugal contacts the descending process of the postorbital, which overlaps the former in the

orbital margin (Fig. 3), as in the holotype of *T. riograndensis* (Oliveira *et al*. 2010) and *E. lunensis* (PVSJ 481).

Interparietal. This bone is likely observable in dorsal, lateral, and occipital views, with only a small portion of its right dorsal edge missing (Figs. 4, 6). However, it is not possible to observe its sutures with the other bones, and so its limits must remain conjectural. In dorsal view, the interparietal of CAPPA/UFSM 0029 contributes to the posterior end of the sagittal crest and participates in the posterodorsal portion of the occipital crest, as the holotype UFRGS PV-1051-T (see Oliveira *et al*. 2010). As in *T. riograndensis* (UFRGS PV-1051-T) and in *E. lunensis*, two concavities are visible in occipital view, in the area supposedly close to the contact with the tabulars.

Squamosal. The squamosal of CAPPA/UFSM 0029 is poorly preserved, and the sutures that delimit this bone are not observable (Figs. 2-4, 6-7). This element is greatly damaged in both sides and the zygomatic arches are fragmented on the contact between squamosal and jugal (Figs. 2-3). The left squamosal is better preserved than the right one (Figs. 2-3). The area of articulation of the skull with the jaw is damaged. However, there is a small element that might correspond to quadrate/quadratojugal (Fig. 3).

The squamosal also forms the anteroventral portion of the occipital crest and a small ventral part of the posterior region of the skull (Figs. 4, 7). In CAPPA/UFSM 0029 and in the holotype of *T. riograndensis*, the pterygoparoccipital foramen opens anteriorly into the temporal fossa. In *E. lunensis* this foramen is closed by the quadrate ramus of the epipterygoid. Due to the state of preservation of CAPPA/UFSM 0029 in this region, the visualization of the sutures is not completely possible. In the lateral surface of the squamosal, there is a dorsoventral sulcus (external auditory meatus) (Figs. 2-3) and, at the posterior end, this bone participates in the occipital crest. The squamosal also forms the posterior portion of the lateral wall of the occipital

crest, in occipital view (Fig. 6). The squamosal extensively contacts the tabular and these bones delimitate the posterior opening of the post-temporal foramen, as in *T. riograndensis* (UFRGS PV-1051-T) (Oliveira *et al*. 2010). Conversely, in *E. lunensis* this opening is surrounded entirely by the tabular bone.

Unfortunately, the visualization of the sutures of the squamosal with the surrounding bones is impossible in CAPPA/UFSM 0029, preventing the observation if it contributes only to the posterior portion of the lateral wall of the occipital crest, as in the holotype UFRGS PV-1051-T, or if it contributes also to the posterolateral portion of the sagittal crest, as in *E. lunensis* and *Probainognathus* (Martínez *et al*. 1996).

Tabular. CAPPA/UFSM 0029 preserves both tabulars (Fig. 6). They form the dorsolateral part of the occiput and, together with the squamosal, contribute to the dorsolateral and lateral margins of the occipital crest, as in *T. riograndensis* (UFRGS PV-1051-T) and *E. lunensis* (Martínez *et al*. 1996; Oliveira *et al*. 2010). The tabular contacts the interparietal dorsomedially and the squamosal laterally, but the exact sutural contacts with the surrounding elements are not clear.

Supraoccipital. In occipital view, the supraoccipital of CAPPA/UFSM 0029 delimits almost the entire dorsal margin of the foramen magnum. This element contacts the interparietal dorsally, and the tabulars laterally (Fig. 6). The contact with the exoccipital is obscured by incrustation. The foramen magnum is relatively large and triangular in outline (Fig. 6). In *E. lunensis,* the foramen magnum is oval-shaped, whereas in UFRGS PV-1051-T it is modified by the diagenesis. The ventral margin of the foramen magnum of CAPPA/UFSM 0029 (Fig. 7), in both the posterior portion of the parabasisphenoid complex and almost all basioccipital are either missing or suffered damages, exposing an internal portion of the braincase.

Exoccipital. Both exoccipital bones are complete, located ventrolaterally to the foramen magnum. The exoccipitals are elongated and their extremities form bulbous occipital condyles. As well as in other ecteniniids, the exoccipital completely form the occipital condyles. These elements cannot be observed in dorsal view, as they are covered by the posteriorly expanded occipital crests, such as in UFRGS PV-1051-T and *E. lunensis.* This feature differs from the generally observed condition in non-ecteniniid eucynodonts, in which they are exposed in dorsal view [e.g., *Lumkuia fuzzi*, *Massetognathus ochagaviae* Barberena, 1981 (UFRGS PV-0255-T)]. The occipital condyles delimit the foramen magnum in their lateral and ventral margins. The exoccipital contacts the supraoccipital dorsally, the paroccipital process of the opisthotic laterally, and the preserved portion of the basioccipital medioventrally. Below the contact with the preserved portion of the basioccipital, this later element anteriorly contacts the parabasisphenoid complex, which is visible ventrally. In CAPPA/UFSM 0029 and UFRGS PV-1051-T, the hypoglossal foramen is not visible, but the jugular foramen is present in the second specimen. In *E. lunensis*, a small hypoglossal foramen is located below the occipital condyles and posteromedially to the jugular foramen (Martínez *et al*. 1996).

Pterygoid. In spite of the bad preservation of the ventral aspect of the new specimen, the pterygoid is almost complete, but significantly affected by taphonomic deformation (Fig. 7). Anterior to the pterygoid, the bones of the secondary palate are missing. The posterior portion of the pterygoid is broken on the contact with the parabasisphenoid complex, where visualization of sutures is not possible given the poor preservation of this region (Fig. 7). The pterygoid flanges are long, narrow, subtriangular in ventral view, and taper ventrally. On the other hand, in UFRGS PV-1051-T they are more expanded laterally and stout, with a triangular-shaped cross section (Oliveira *et al*. 2010). In *E. lunensis*, the pterygoid flanges are quadrangular, broad and robust, extended backwards behind the orbits, as their tips curve posteromedially (Martínez *et al*. 1996).

The pterygoid of *E. lunensis* forms three ridges, one median and two lateral, radiating forward from a point at the front of the basisphenoid (Martínez *et al*. 1996). In the new specimen and in the holotype of *T. riograndensis*, this region is damaged, which prevents confirmation of such ridges.

Parabasisphenoid complex. Taphonomic deformation strongly affected the parabasisphenoid complex of CAPPA/UFSM 0029 (Fig. 7). The complex is placed in the medial portion of the basicranium and has an elongated triangular shape. In the anterior portion, the basisphenoid is broken close to the contact with the pterygoids and its almost entire posterior portion is missing or damaged. In this region, due to its poor preservation, it is not possible to observe the contact of the basioccipital with the posterior portion of the basicranium and to the ventral rim of the foramen magnum. In CAPPA/UFSM 0029 and *T. riograndensis* (UFRGS PV-1051-T) the parabasisphenoid complex presents a low median parabasisphenoid ridge and two well-developed basisphenoid wings laterally (Oliveira *et al*. 2010). In the medial portion of this element, there is a fracture that obscures details of this region in CAPPA/UFSM 0029. In the new specimen, in the holotype of *T. riograndensis*, and in *E. lunensis*, the parabasisphenoid lacks foramina for the internal carotids (Martínez *et al*. 1996; Oliveira *et al*. 2010).

Prootic and Epipterygoid. Both elements are taphonomically affected and their sutures are uncertain. The prootic is observable in lateral and ventral views (Figs. 6-7), although the contacts with other bones are not visible. A large and round post-temporal foramen is anteroventrally opened, between the prootic and epipterygoid (Fig. 6). In ventral view, the prootic contacts the parabasisphenoid complex medially and the squamosal posteriorly. The epipterygoid of CAPPA/UFSM 0029 is visible in lateral view.

Mandible. The lower jaw preserves the anterior and middle portions of both dentaries, whereas posterodorsally it is damaged in some degree (Figs. 2-3). The mandibular symphysis is

fused, anteroposteriorly sloped and dorsoventrally convex on its anterior portion. The angular and coronoid processes of CAPPA/UFSM 0029 are posteriorly damaged. Its postdentary elements are partially preserved. The lower jaw of *T. riograndensis* (holotype UFRGS PV-1051-T) is better preserved than in CAPPA/UFSM 0029, so the former specimen provides more information the about postdentary bones and lower dentition.

The dentary is long, deep, and robust (Figs. 2-3). As already mentioned, the dentaries are fused at the mandibular symphysis, which posteriorly extends to the anterior level of the upper canine tooth. The fused symphysis is typical for most non-mammaliamorph eucynodonts, except in more derived forms (see Bonaparte 1980; Bonaparte *et al*. 2001; Martinelli *et al*. 2016b). The body of the dentary is almost uniformly deep along its length (Figs. 2-3), as in the holotype of *T. riograndensis* (see Oliveira *et al*. 2010).

The posterodorsal portions of the both coronoid processes are damaged, but the left dentary is better preserved than the right one (Figs. 2-3). The coronoid process of CAPPA/UFSM 0029 is broad and deep, posteriorly extending beyond the level of the angular process, as in the holotype of *T. riograndensis* (see Oliveira *et al*. 2010). In comparison, the coronoid process of *E. lunensis* is thin and tall, with its anterior margin slightly concave, and its dorsal border reaching the top of the sagittal crest when articulated to the skull (Martínez *et al*. 1996). In *Chiniquodon sanjuanensis* (PVSJ 411), this structure is also tall and reaches the level of the sagittal crest (Martínez & Forster 1996). In most gomphodontians, such as the traversodontid *Exaeretodon riograndensis*, the coronoid process is greatly developed and taller than in probainognathians (Liparini *et al*. 2013).

A shallow and broad masseteric fossa extends anteroposteriorly on the lateral of the body of the dentary (Figs. 2-3). In CAPPA/UFSM 0029, UFRGS PV-1051-T, and *E. lunensis* (PVSJ 481), the masseteric fossa occupies almost entirely the lateral surface of the posterior half of

dentary (see Oliveira *et al*. 2010). In comparison, in the holotype of *E. lunensis* (PVSJ 422) it is slightly less wide (Martínez *et al*. 1996). In the new specimen, this structure begins behind the last postcanine, as in the holotype of *T. riograndensis* (Oliveira *et al*. 2010). In other cynodont groups, such as in *Diademodon tetragonus* Seeley, 1894, the masseteric fossa extends well forward, until the level of the sixth lower postcanine (Martinelli *et al*. 2009) and in *Chaliminia musteloides* Bonaparte, 1980 the masseteric fossa is broad, developed on the entire lateral surface of the coronoid process, and anteriorly extended to the level of the last upper postcanine (Martinelli & Rougier 2007).

The lateral surface of the anterior region of the dentary of CAPPA/UFSM 0029 is perforated by the mental foramen, which is located at the level of the first upper postcanines (Figs. 2-3). In the holotype of *T. riograndensis*, this foramen is close to the level of the third postcanine (see Oliveira *et al*. 2010). *E. lunensis* presents two foramina, the first one larger, located immediately behind the upper canine and a second one smaller and dorsolaterally placed beneath the third postcanine (Martínez *et al*. 1996). The Meckelian groove of CAPPA/UFSM 0029 is not visible.

The tip of the angular process is lacking in both dentaries of CAPPA/UFSM 0029. In the holotype UFRGS PV-1051-T, the angular process has a posteriorly projected tip (Oliveira *et al*. 2010). In most of the traversodontids this often process is prominent and acute (Liparini *et al*. 2013). In CAPPA/UFSM 0029, the dentary ends near the jaw articulation, as in *T. riograndensis* (UFRGS PV-1051-T).

In both sides of the lower jaw, the postdentary bones are partially preserved, comprising a fragile structure in the posterior end of the dentary (Figs. 2-3, 7). They are located medially and posterodorsally to the angular process, and ventrally to the level of the preserved portions of the coronoid process. The postdentary bones are not easily identifiable because of the bad

preservation and their sutures are not clear. The left angular, surangular, and prearticular are preserved, whereas only parts of the right angular and surangular are clearly identifiable. In ventral view, both right and left angular bones are partially visible. The angular articulates between the surangular and prearticular, dorsally contacting the preserved portion of the surangular and, lateroventrally, the preserved portion from prearticular. The angular forms an anteroposteriorly long bar, which extends medially and posterodorsally to the level of the angular process. The angular and surangular are apparently unfused and a putative contact is observable between these bones, as in the holotype of *T. riograndensis* (UFRGS PV-1051-T) (see Oliveira *et al*. 2010) (Figs. 3, 7). In UFRGS PV-1051-T, the postdentary bones form a long and slender bar that extends below the medial crest of the dentary (Oliveira *et al*. 2010). The angular plus surangular of the holotype of *T. riograndensis* are partially parallel to each other, extended medially behind the angular process, and contact the prearticular and articular posterodorsally.

The surangular, visible on the lateral view of both sides of the lower jaw, is better preserved in the left side of the specimen (Figs. 2-3). The anterior portion from the surangular forms a bar with tapered ends with an angle of about 45º in relation to the main axis of the body of the dentary. The left prearticular is incomplete, whereas the right one is missing. In ventral view, the contact between the prearticular and angular is clearly observable, as in *T. riograndensis* (UFRGS PV-1051-T). Unfortunately, both articular and retroarticular processes are not preserved.

Dentition. As the lower jaw is in occlusion, the lower dentition is not exposed (Figs. 2-3, 5, 8). In contrast to the condition in other ecteniniids, serrations cannot be observed in any tooth, although this may be due to poor preservation (Figs. 2-3). The upper left dentition presents a dental formula of four incisors (Figs. 5, 8), one canine, and five preserved postcanines, but with space for up to eight postcanine teeth (Figs. 2-3). The upper right dentition shows the same

formula of incisors and canines, but postcanines are not preserved. The upper dental formula 4I/1C/8PC is present in the holotype of *T. riograndensis* and *E. lunensis* (Martínez *et al*. 1996; Oliveira *et al*. 2010), whereas it is 4I/1C/7PC in *D. elegans* (Martínez *et al*. 2013). However, changes in the number of postcanines along ontogeny are not known in ecteniniids due to the limited sample of specimens, but difference in postcanine numbers along different stages is frequent in cynodonts (Fourie 1963).

The upper incisors are thin and long (Fig. 4), with the first right one being smaller than the following and successively larger teeth. The left side presents the same condition, however the first incisor is slightly smaller than the following ones. The posterior increase in size of the incisors is shared with the holotype UFRGS PV-1051-T, but different from *E. lunensis* (PVSJ 422), in which the first two incisors are the longest and thinnest. The root of the fourth right incisor of CAPPA/UFSM 0029 is exposed due to damage to the maxilla. This tooth, as well as the last two left incisors, are slightly damaged in their tip.

In CAPPA/UFSM 0029 and UFRGS PV-1051-T the third and fourth premaxillary teeth are slightly more spaced from each other than the remaining ones (see Oliveira *et al*. 2010), in contrast to *E. lunensis*, in which the incisors are evenly spaced. In *D. elegans* the incisors are unevenly located and the two posterior teeth are more spaced in comparison to the anterior ones (Martínez *et al*. 2013). As in the other ecteniniids, the four incisors of CAPPA/UFSM 0029 are implanted in the premaxilla. This bone enters medially to the anteroventral portion of the maxilla and the fourth incisor seems to be in the maxilla.

CAPPA/UFSM 0029 lacks visible serrations on the incisors (Fig. 4), although this is possibly an artifact of preservation. In *E. lunensis* the serrations are absent (Martínez *et al*. 1996), whereas in UFRGS PV-1051-T the distal margin of the last three incisors are serrated and on the lingual side there is a high vertical ridge in the fourth incisor (Oliveira *et al*. 2010). In the new

specimen, the lingual side is not visible. As in the other ecteniniids, the labial surface of the incisors is flat and possess longitudinal striations, mainly in the two posterior teeth, a condition found in *E. lunensis* and *D. elegans* (Martínez *et al*. 1996; 2013).

A slight procumbent orientation of the incisors is present in CAPPA/UFSM 0029, but this feature can possibly be due to laterodorsal compression that anteriorly displaced them forwards. Procumbent incisors are also present in *E. lunensis* (Martínez *et al*. 1996), whereas in other probainognathian cynodonts (e.g., UFRGS PV-1051-T, *D. elegans*, *Chiniquodon sanjuanensis*, *Probainognathus jenseni*, *Lumkuia fuzzi*) a vertical or slightly recumbent orientation is prevalent.

In CAPPA/UFSM 0029, the upper canines are long, well developed, labiolingually compressed, and slightly recurved backwards (Figs. 2-3, 5, 8). Both are practically complete, with only a small portion of each tip missing. The canines are quite long and almost reach the ventral margin of the dentary. As in other ecteniniids, the cross-section of the canine is round near its implantation in the maxilla and becomes more oval towards its tip (Martínez *et al*. 1996; 2013).

CAPPA/UFSM 0029 and the other ecteniniids present an anterior diastema, between the last incisor and the canine. The upper canines do not present visible serrations, but as with the incisors, this is possibly an artifact of preservation. *D. elegans* lacks serrations on the preserved fragments of its functional canines as well as on the replacement canines, but these are badly preserved as well (Martínez *et al*. 2013). Conversely, in *E. lunensis* the canines are finely serrated along their length (Martínez *et al*. 1996), and in UFRGS PV-1051-T the distal margin bears a conspicuous serration, whereas in the mesial border, serrations are visible only near the tip of the tooth (Oliveira *et al*. 2010). As in the other ecteniniids, CAPPA/UFSM 0029 shows a small diastema between the canine and the first upper postcanine (Figs. 2-3).

The upper postcanines of CAPPA/UFSM 0029 are preserved only in the left side of the specimen, but they are little exposed and their dental anatomy is poorly preserved (Fig. 3). There are five mesiodistally-aligned postcanines exposed or partially exposed in the maxilla. The first one has only one main cusp visible, however the distal margin of the tooth is damaged. Behind of the first postcanine there is a gap, large enough to accommodate three teeth (second to fourth postcanines). This gap visibly present a healed bone, indicating natural teeth loss. The supposed fifth, sixth, and seventh postcanines are more exposed and complete than the others, being longitudinally aligned, with two well-recurved and posteriorly directed cusps: one large mesial main cup and other smaller accessory distal one. Whereas the new specimen exposes only these two cups, in other ecteniniids these same elements present three to four cusps. The fifth to seventh postcanines are subequal in size. The eighth tooth is damaged, precluding access to its morphology.

The left side of the specimen PVSJ 481 of *E. lunensis*, which is affected by similar lateral compression as CAPPA/UFSM 0029, has a similar dental morphology. The last upper postcanines, fifth to seventh, are more exposed than the others, and present two cusps, one main, large and other small accessory. However, in the right side of PVSJ 481, which is not affected by compression, the teeth have three cusps preserved.

As in other ecteniniids, the postcanines (fifth to seventh) of CAPPA/UFSM 0029 are evidently sectorial. In CAPPA/UFSM 0029 and all other ecteniniids, all teeth are in contact to each other, forming an imbricated dentition with backwardly directed cusps (Fig. 3). In *T. riograndensis* (UFRGS PV-1051-T) and *E. lunensis* the four anterior postcanines are smaller than the four posterior ones, these last presenting mesial main cusps larger than the accessory ones, with their mesial margin posteriorly recurved (Martínez *et al*. 1996; Oliveira *et al*. 2010). *D. elegans* preserves only the fourth postcanine, which presents a complete crown with four cusps

(Martínez *et al*. 2013). The recurved pattern of the mesial margin resembles the condition found in other ecteniniids and chiniquodontids.

CAPPA/UFSM 0029 lacks serrations on any of its postcanine teeth. In the holotype of *T. riograndensis*, all the cusps have mesial and distal margins serrated except by the mesial edge of the main cusp of the five first postcanines (Oliveira *et al*. 2010). In *E. lunensis* the cusps of all postcanines are serrated in both edges (Martínez *et al*. 1996), and in *D. elegans* the only preserved postcanine (fourth), lacks serrations (Martínez *et al*. 2013).

As the mandible is in position of articulation with the skull, the lower dentition of CAPPA/UFSM 0029 is hidden by the upper cheek teeth series and the maxilla, with only a small anterior portion of the left canine visible. Using computed tomography to access the internal anatomy of the specimen (Fig. 8), it was possible to identify the presence of three lower incisors and at least seven postcanines. The lower canines are also observable inside the paracanine fossa with their tips slightly protruding through the skull roof, however are not visible in the dorsal surface. Unfortunately, no other details were possible to access through computed tomography. Among ecteniniids, the lower dentition of UFRGS PV-1051-T presents a dental formula 3i/1c/8pc, although in *E. lunensis* (PVSJ 422) the lower dentition is unknown because the lower jaw is completely occluded (Martínez *et al*. 1996; Oliveira *et al*. 2010).

Phylogenetic analysis

The analysis recovered two MPCs of 458 steps each (CI = 0.469; RI = 0.785; RC = 0.368), and the consensus is shown in Figure 9. CAPPA/UFSM 0029 was recovered as the sister-group of *Trucidocynodon riograndensis* (UFRGS PV-1051-T) in both MPCs, supported by the extranasal process of the premaxilla large but not contacting the nasal (state 1 of the character 1). This node lies within the clade Ecteniniidae, and, in the strict consensus cladogram, CAPPA/UFSM 0029

plus the holotype UFRGS PV-1051-T form a trichotomy with *Diegocanis elegans* and *Ecteninion lunensis* (Fig.9).

Ecteniniidae is supported by nine synapomorphies, most of them scored as missing data in the new specimen. Yet, some observable traits of this node are clearly present in CAPPA/UFSM 0029 and include: (i) the temporal fossa with constant width along its length (state 1 of the character 23); (ii) angle of dentary close to jaw joint (state 1 of the character 84); and (iii) length of the temporal region longer than the length of the sagittal crest (state 0 of the character 147). Other features supporting the clade Ecteniniidae, although missing in the new specimen, are related to a short osseous secondary palate, the space for trigeminal ganglion partly floored by prootic, presence of serrations in canine teeth, strongly developed acromion process of the scapula, and absence of ectepicondylar foramen in the humerus. The general topology of the MPCs also reveals some differences from those produced by Liu & Olsen (2010) and Martinelli *et al*. (2016b). *Lumkuia fuzzi* is herein recovered as the basalmost member of Probainognathia, agreeing with Hopson & Kitching (2001) and Martínez *et al*. (2013). On the other hand, Martinelli *et al*. (2016b) recovered this taxon as the basalmost eucynodont, therefore, basal to the Cynognathia – Probainognathia dichotomy. In Martinelli *et al*. (2016b), *E. lunensis* is placed as the basal most member of Probainognathia. Nevertheless, in our results, it is more derived than *Chiniquodon* and *Probainognathus*, placed within Ecteniniidae, as the sister-group of Prozostrodontia.

Final Remarks

The Janner outcrop has produced an important suite of fossil vertebrates (Oliveira *et al*. 2007; Cabreira *et al*. 2011; Liparini *et al*. 2013; Müller *et al*. 2015; Pretto *et al*. 2015; Martinelli *et al*. 2016b), including the large carnivorous non-mammaliaform probainognathian, *Trucidocynodon*

riograndensis (Oliveira *et al*. 2010). More recently, the specimen CAPPA/UFSM 0029 described herein was recovered from this outcrop. The new specimen is phylogenetically closer to *T. riograndensis* to any than other ecteniniid, it is in a sister-group relationship with the holotype of *T. riograndensis,* and both are in a trichotomy with *Diegocanis elegans* and *Ecteninion lunensis*, nested within the monophyletic Ecteniniidae. CAPPA/UFSM 0029 sharing with the holotype UFRGS PV-1051-T a unique combination of features that permits its referral to *T. riograndensis*, as follows:

(i) Extranasal process of the premaxilla large but not contacting the nasal. In *Ecteninion lunensis* and *Diegocanis elegans*, this process is less developed comparatively;

(ii) Pterygoparoccipital foramen anteriorly opened. In *E. lunensis*, the foramen is closed by the quadrate ramus of the epipterygoid. In *D. elegans,* this feature is unknown;

(iii) Posterior opening of the post-temporal foramen limited by the tabular and the squamosal. In *E. lunensis*, the posterior opening of the post-temporal foramen is totally enclosed by the tabular. In *D. elegans,* this feature also is unknown;

(iv) External opening of the paracanine fossa. In the new specimen, in the holotype of *T. riograndensis,* and in *E. lunensis* a dorsal opening allow the lower canines to protrude through the snout roof, whereas in *D. elegans* there is no dorsal opening of the paracanine fossae.

CAPPA/UFSM 0029 is approximately 17% larger than the holotype of *T. riograndensis*, as its maximum anteroposterior skull length is 225 mm, whereas UFRGS PV-1051-T reaches 187.5 mm (Table 1). In contrast, Argentinean ecteniniid taxa from the Ischigualasto Formation are much smaller. The holotype of *E. lunensis* presents a total skull length of 98.4 mm, which is approximately 56.25% smaller than the new specimen of *T. riograndensis* and the holotype of *D.*

elegans in which the preserved cranial length (53.9 mm) is approximately 58.85% less than CAPPA/UFSM 0029.

The new large specimen of *T. riograndensis* increases the number of specimens of ecteniniids in the Upper Triassic of Southern Brazil (Santa Maria Supersequence, Candelária Sequence, Late Carnian). In addition, CAPPA/UFSM 0029 is larger than the holotype, and as far as we know, it represents one the largest Late Triassic carnivorous probainognathian, contributing to the knowledge of size variation of ecteniniids.

Acknowledgements

The authors thank Cesar L. Schultz and Marina B. Soares (UFRGS) who allowed access to the collection under their care; Agustín G. Martinelli, Tomaz P. Melo (UFRGS), and Diego Abelin (PVSJ) for their assistance during the visit to the collections; medical clinic Dix (Diagnóstico por Imagem do Hospital de Caridade, Santa Maria, Rio Grande do Sul) for kindly allow access to their CT-Scan. This work was supported by the Coordenação de Aperfeiçoamento de Pessoal de Nível Superior (CAPES) scholarship for MS and RTM, Fundação de Amparo à Pesquisa do Estado do Rio Grande do Sul (FAPERGS 17/2551-0000816-2) to LK, and by Conselho Nacional de Desenvolvimento Científico e Tecnológico (CNPq, 306352/2016-8) to SDS. We also extend our gratitude to the Willi Henning Society, for the gratuity of TNT software.

References

Abdala, F., Barberena, M.C. & Dornelles, J. (2002) A new species of the traversodontid cynodont *Exaeretodon* from the Santa Maria Formation (Middle/Late Triassic) of Southern Brazil. *Journal of Vertebrate Paleontology*, 22, 313–325.

Abdala, F. & Ribeiro, A.M. (2010) Distribution and diversity patterns of Triassic cynodonts (Therapsida, Cynodontia) in Gondwana. *Palaeogeography, Palaeoclimatology, Palaeoecology*, 286, 202–217.

Barberena, M.C. (1981) Uma nova espécie de *Massetognathus* (*Massetognathus ochagaviae*, sp. nov.) da Formação Santa Maria, Triássico do Rio Grande do Sul. *Pesquisas*, 14, 181–195.

Bonaparte, J.F. (1980) El primer ictidosaurio (Reptilia – Therapsida) de América del Sur, *Chaliminia musteloides*, del Triásico Superior de La Rioja, República Argentina. *In: 2nd Congreso Argentino de Paleontología y Bioestratigrafía y 1st Congreso Latinoamericano de Paleontología, Actas.* Buenos Aires, Argentina, 1, 123–133.

Bonaparte, J.F., Ferigolo, J. & Ribeiro, A.M. (2001) A primitive Late Triassic "ictidosaur" from Rio Grande do Sul, Brazil. *Palaeontology*, 44, 623–635.

Bonaparte, J.F. & Migale, L.A. (2015) *Protomamíferos y Mamíferos Mesozoicos de América del Sur.* Museo de Ciencias Naturales Carlos Ameghino, Mercedes, Argentina, 422 pp.

Broom, R. (1905) Preliminary notice of some new fossil reptiles collected by Mr. Alfred Brown at Aliwal North, South Africa. *Records of the Albany Museum*, 1, 269–275.

Broom, R. (1937) A further contribution to our knowledge of the fossil reptiles of the Karroo. *Proceedings of the Zoological Society of London*, 107, 299–318.

Cabreira, S.F., Schultz, C.L., Bittencourt, J.S., Soares, M.B., Fortier, D.C., Silva, L.R. & Langer, M.C. (2011) New stem-sauropodomorph (Dinosauria, Saurischia) from the Triassic of Brazil. *Naturwissenschaften*, 98, 1035–1040.

Fonseca, M.M. (1999) *Caracterização faciológica das Formações Santa Maria (Membro Alemoa) e Caturrita: Interpretação da tipologia de sistemas fluviais* (M.S. thesis). Universidade Federal do Rio Grande do Sul (unpublished).

Fourie, S. (1963) Tooth replacement in the gomphodont cynodont, *Diademodon*. *South African Journal of Science,* 59, 211–213.

Goloboff, P.A., Farris, J.S. & Nixon, K.C. (2008) TNT, a free program for phylogenetic analysis. *Cladistics*, 24, 774–786.

Hilleniuws, J. (2000) Septomaxilla of nonmammalian synapsids: softtissue correlates and a new functional interpretation. *Journal of Morphology*, 245, 29–50.

Hopson, J.A. & Kitching, J.W. (2001) A probainognathian cynodont from South Africa and the phylogeny of nonmammalian cynodonts. *Bulletin of the Museum of Comparative Zoology*, 156, 5–35.

Hopson, J.A. (1990) Cladistic analysis of therapsid relationships. *Journal of Vertebrate Paleontology*, 10, 28pp.

Horn, B.L.D., Melo, T.M., Schultz, C.L., Philipp, R.P., Kloss, H.P. & Goldberg, K. (2014) A new third-order sequence stratigraphic framework applied to the Triassic of the Paraná Basin, Rio Grande do Sul, Brazil, based on structural, stratigraphic and paleontological data. *Journal of South American Earth Sciences*, 55, 123–132.

Huene, F.F. von (1936) *Die Fossilien Reptilien des Südamerikanischen Gondwanalands.* C.H. Beck'sche Verlag, Münich, 332 pp.

Huxley, T.H. (1859) Postscript to: On the sandstones of Morayshire (Elgin & c.) containing reptile remains, and their relations to the Old Red Sandstone of that country. *Quarterly Journal of the Geological Society of London,* 15, 138–152.

Kemp, T.S. (1982) *Mammal-like Reptiles and the Origin of Mammals.* Academic Press, London, 363 pp.

Langer, M.C., Ribeiro, A.M., Schultz, C.L. & Ferigolo, J. (2007) The continental Tetrapod bearing Triassic of South Brazil. *Bulletin of the New Mexico Museum of Natural History and Science*, 41, 201–218.

Langer, M.C., Ramezani, J. & Da Rosa, Á.A. (2018) U-Pb age constraints on dinosaur rise from south Brazil. *Gondwana Research*, 57, 133–140.

http://dx.doi.org/10.1016/j.gr.2018.01.005

Liparini, A., Oliveira, T.V., Pretto, F.A., Soares, M.B. & Schultz, C.L. (2013) The lower jaw and dentition of the traversodontid *Exaeretodon riograndensis* Abdala, Barberena & Dornelles, from the Brazilian Triassic (Santa Maria 2 Sequence, *Hyperodapedon* Assemblage Zone). *Alcheringa*, 37, 1–23.

Liu, J., Soares, M.B. & Reichel, M. (2008) *Massetognathus* (Cynodontia, Traversodontidae) from the Santa Maria Formation of Brazil. *Revista Brasileira de Paleontologia*, 11, 27–36.

Liu, J. & Olsen, P.E. (2010) The phylogenetic relationships of Eucynodontia (Amniota, Synapsida). *Journal of Mammalian Evolution*, 17, 151–176.

Martinelli, A.G. & Rougier, G.W. (2007) On *Chaliminia musteloides* (Eucynodontia: Tritheledontidae) from the Late Triassic of Argentina, and a phylogeny of Ictidosauria. *Journal of Vertebrate Paleontology*, 27, 442–460.

Martinelli, A.G., Fuente, M. & Abdala, F. (2009) *Diademodon tetragonus* Seeley, 1894 (Therapsida: Cynodontia) in the Triassic of South America and its biostratigraphic implications. *Journal of Vertebrate Paleontology*, 29, 852–862.

Martinelli, A.G. & Soares, M.B. (2016) Evolution of South American cynodonts. *Contribuciones Científicas del Museo Argentino de Ciencias Naturales "Bernardino Rivadavia"*, 6, 183–197.

Martinelli, A.G., Soares, M.B., Rodrigues, P. & Schultz, C.L. (2016a) The oldest ictidosaur cynodont (Therapsida) from the late Carnian of southern Brazil and its implication in probainognathian evolution. *In: X Simpósio Brasileiro de Paleontologia de Vertebrados, Rio de Janeiro.* Boletim de resumos, 111 pp.

Martinelli, A.G., Soares, M.B. & Schwanke, C. (2016b) Two new cynodonts (Therapsida) from the Middle-Early Late Triassic of Brazil and comments on South American probainognathians. *Plos One*, 11(10).

http://dx.doi.org/10.1371/journal.pone.0162945

Martínez, R.N. & Forster, C.A. (1996) The skull of *Probelesodon sanjuanensis*, sp. nov., from the Late Triassic Ischigualasto Formation of Argentina. *Journal of Vertebrate Paleontology*, 16, 285–291.

Martínez, R.N., May, C.L. & Forster, C.A. (1996) A new carnivorous cynodonts from the Ischigualasto Formation (Late Triassic, Argentina), with comment on eucynodont phylogeny. *Journal of Vertebrate Paleontology*, 16, 271–284.

Martínez, R.N., Fernandez, E. & Alcober, O.A. (2011) A new advanced eucynodont (Synapsida, Cynodontia) from the Carnian-Norian Ischigualasto Formation, northwestern Argentina. *Ameghiniana*, 48, R109 pp.

Martínez, R.N., Fernandez, E. & Alcober, O.A. (2013) A new nonmammaliaform eucynodont from the Carnian-Norian Ischigualasto Formation, northwestern Argentina. *Revista Brasilera de Paleontología*, 16, 61–76.

Müller, R.T., Langer, M.C., Aires, A. & Dias-da-Silva, S. (2014) New dinosauriform (Ornithodira, Dinosauromorpha) record from the Late Triassic of Southern Brazil. *Paleontological Research*, 18, 118–121.

Müller, R.T., Araújo-Junior, H.I., Aires, A.S.S., Roberto-da-Silva, L. & Dias-da-Silva, S. (2015) Biogenic control on the origin of a vertebrate monotypic accumulation from the Late Triassic of Southern Brazil. *Geobios,* 48, 331–340.

Müller, R.T., Langer, M.C., Cabreira, S.F. & Dias-da-Silva, S. (2016) The femoral anatomy of *Pampadromaeus barberenai* based on a new specimen from the Upper Triassic of Brazil. *Historical Biology*, 28, 656–665.

Müller, R.T., Langer, M.C., Pacheco, C.P. & Dias-da-Silva, S. (2017) The role of ontogeny on character polarization in early dinosaurs: a new specimen from the Late Triassic of Southern Brazil and its implications. *Historical Biology*, pp. 1–12.

http://dx.doi.org/10.1080/08912963.2017.1395421

Oliveira, T.V. & Schultz, C.L. (2007) La predominancia de *Exaeretodon* Cabrera 1943 en una sección Triásica de Brasil y su probable correlación con el mismo evento en la porción mediana superior de la Formación Ischigualasto (Triásico de Argentina). *In: 23rd Jornadas Argentinas de Paleontología de Vertebrados, Programa de Comunicaciones Científicas y Libro de Resumenes.* Trelew, Argentina, 9 pp.

Oliveira, T.V., Schultz, C.L. & Soares, M.B. (2007) O esqueleto pós-craniano de *Exaeretodon riograndensis et al*. (Cynodontia, Traversodontidae), Triássico do Brasil. *Revista Brasileira de Paleontologia*, 10, 79–94.

Oliveira, T.V., Soares, M.B. & Schultz, C.L. (2010) *Trucidocynodon riograndensis* gen. nov. et sp. nov. (Eucynodontia), a new cynodont from the Brazilian Upper Triassic (Santa Maria Formation). *Zootaxa,* 2382, 1–71.

Owen, R. (1861) *Palaeontology, or a Systematic Summary of Extinct Animals and their Geological Relationships.* Adam and Black, Edinburgh, 463 pp.

Pretto, F.A., Langer, M.C. & Schultz, C.L. (2015) New dinosaur remains from the Late Triassic of Southern Brazil (Candelária Sequence, *Hyperodapedon* Assemblage Zone). *Alcheringa*, 39, 1–10.

Romer, A.S. (1970) The Chañares (Argentina) Triassic reptile fauna. VI. A chiniquodontid cynodont with incipient squamosal-dentary jaw articulation. *Breviora*, 344, 1–18.

Schultz, C.L., Scherer, C.M.S. & Barberena, M.C. (2000) Bioestratigraphy of Southern Brazilian Middle-Upper Triassic. *Revista Brasileira de Geociências*, 30, 495–498.

Seeley, H.G. (1894) Researches on the structure, organization, and classification of the fossil Reptilia. Part IX, Section 3. On *Diademodon*. *Philosophical Transactions of the Royal Society of London,* 185, 1029–1041.

Sidor, C.A. (2003) The naris and palate of *Lycaenodon longiceps* (Therapsida: Biarmosuchia), with comments on their early evolution in the Therapsida. *Journal of Paleontology*, 77, 977–984.

Soares, M.B., Schultz, C.L. & Horn, B.L.D. (2011) New information on *Riograndia guaibensis* Bonaparte, Ferigolo & Ribeiro, 2001 (Eucynodontia, Tritheledontidae) from the Late Triassic of Southern Brazil: anatomical and biostratigraphic implications. *Anais da Academia Brasileira de Ciências*, 83, 329–354.

Zerfass, H., Lavina, E.L., Schultz, C.L., Garcia, A.J.V., Faccini, U.F. & Chemale, F. JR. (2003) Sequence stratigraphy of continental Triassic strata of Southernmost Brazil: a contribution to Southwestern Gondwana palaeogeography and palaeoclimate. *Sedimentary Geology*, 161, 85–105.

Zerfass, H., Sander, A., Flores, A.E. (2007). Agudo, Folha SH.22-V.C.V, escala 1:100.000, Rio Grande do Sul. Serviço Geológico do Brasil (CPRM), Brasília, 97 pp.

Table 1 – Skull measurements of CAPPA/UFSM 0029 in comparison with the holotype of *Trucidocynodon riograndensis* (UFRGS PV-1051-T). All measurements are given in millimeters (mm). Measurements of *T. riograndensis* and parameters were taken from Oliveira *et al*. (2010).

	CAPPA/UFSM 0029	***Trucidocynodon riograndensis***
Basal skull length	225	187.5
Parietals length on midline	66.6	60.5
Snout length	112.6	84.2
Orbit length	33.1	30.3
Orbit height	22.2	21.0
Postorbital bar anteroposterior thickness	10.3	8.0
Zygomatic arch height	11.1	9.6
Zygomatic arch lateromedial thickness	5.9	4.8
Skull greatest width at occipital plate	85.9	54.8
Skull greatest height at occipital plate	55.6	52.7
Dentary greatest length	150.4	127.7
Dentary greatest height	60.1	62.3
Length of complete upper tooth row	100.1	88.0
Length of postcanine upper tooth row	51.7	44.8
Upper canine height	25.9	23.8

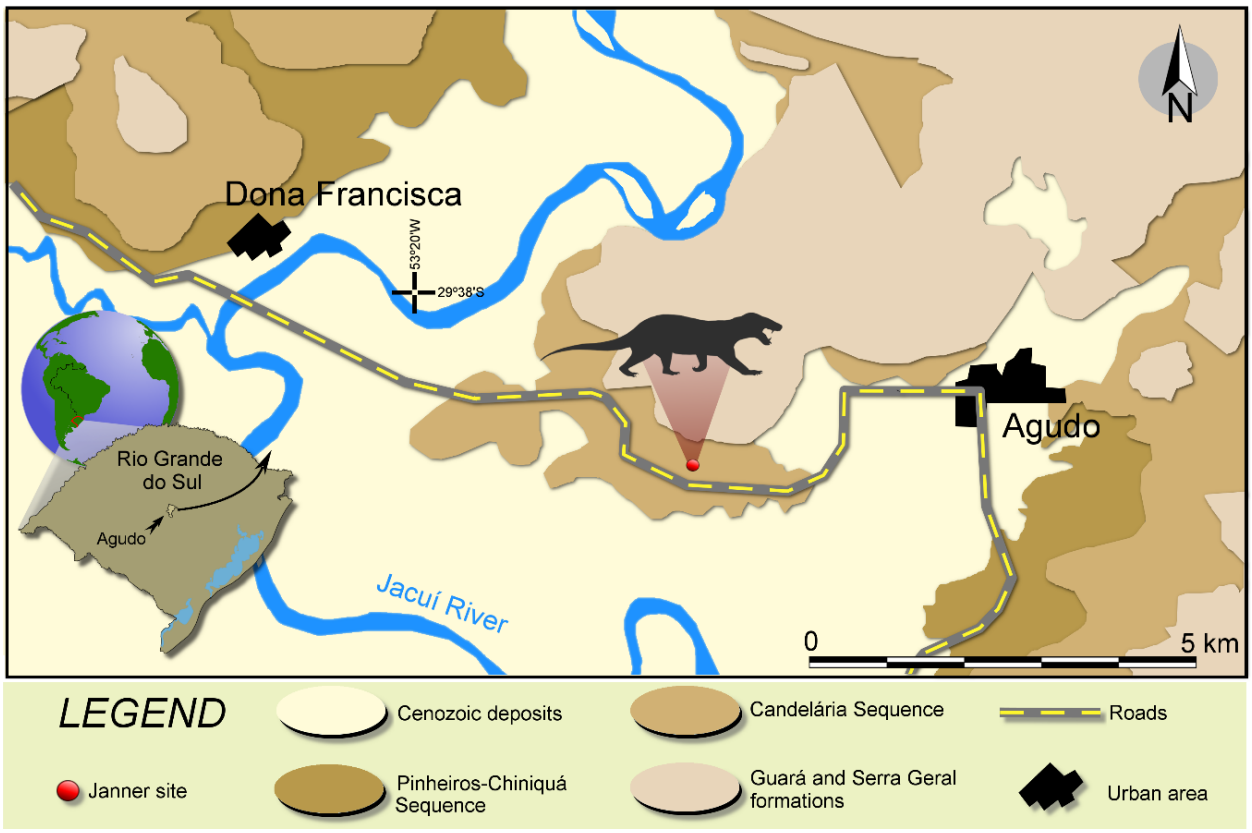

FIGURE 1. Map of the Agudo area, Rio Grande do Sul, Brazil, showing the location of the Janner site (modified from Müller *et al*. 2017). Surface distribution of geological units according to Zerfass *et al*. (2007), with names updated according to Horn *et al*. (2014).

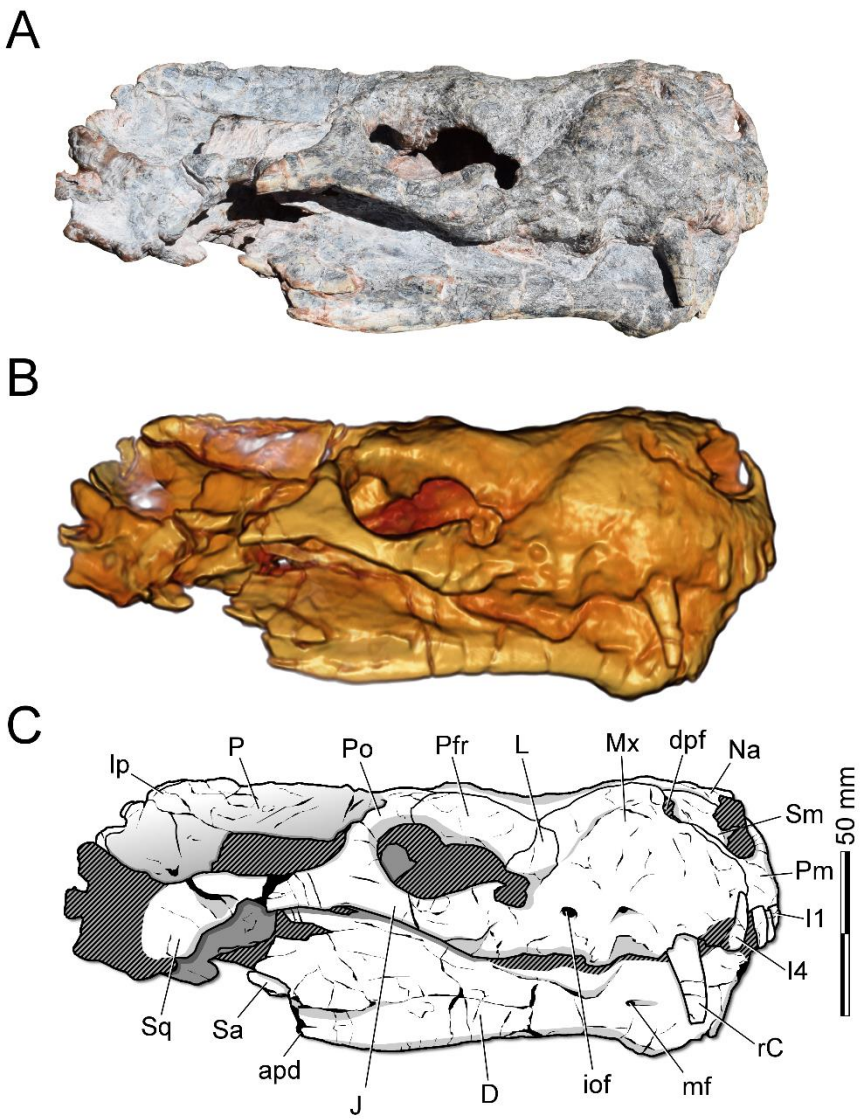

FIGURE 2. Skull and mandible of *Trucidocynodon riograndensis* (CAPPA/UFSM 0029) from the Late Triassic of Southern Brazil, in right lateral view. **A**. photo, **B**. tridimensional model, and **C**. schematic drawing. **Abbreviations: apd**, angular process of the dentary; **D**, dentary; **dpf**, dorsal opening of the paracanine fossa; **I1–4**, upper incisors; **iof**, infraorbital foramen; **Ip**, interparietal; **J**, jugal; **L**, lacrimal; **Mx**, maxilla; **mf**, mental foramen; **Na**, nasal; **P**, parietal; **Pm**, premaxilla; **Po**, postorbital; **Prf**, prefrontal; **rC**, right upper canine; **Sa**, surangular; **Sm**, septomaxilla; **Sq**, squamosal.

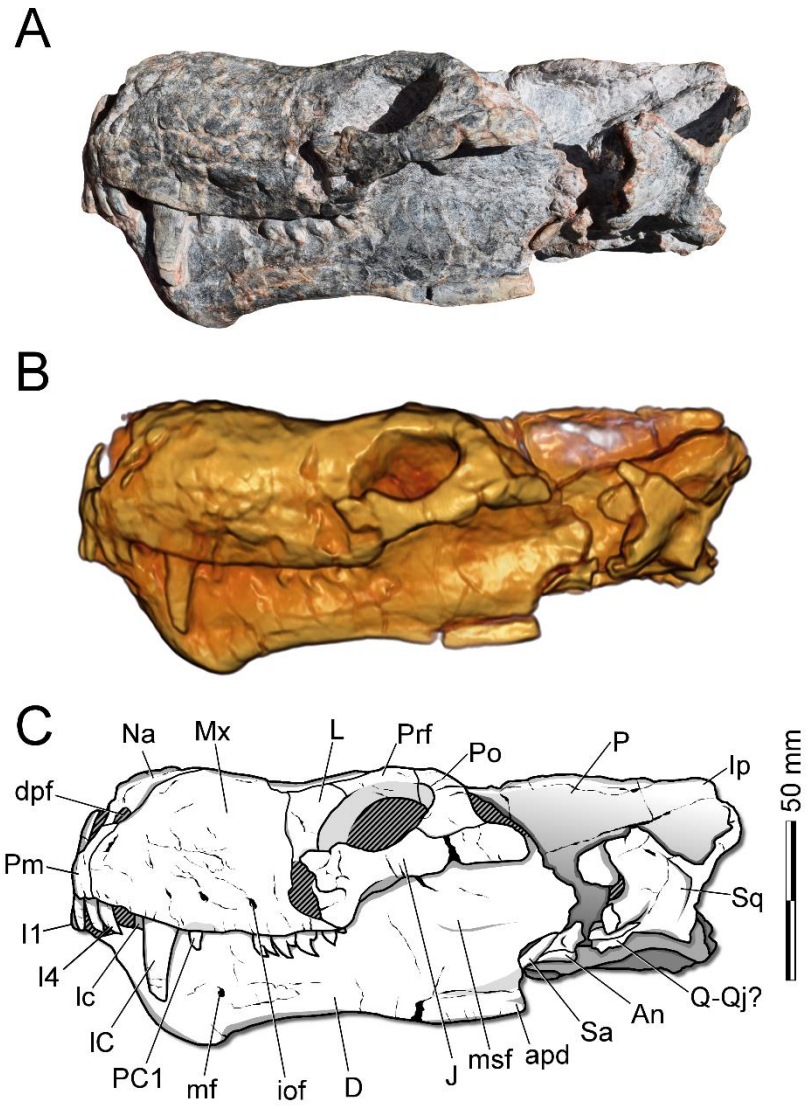

FIGURE 3. Skull and mandible of *Trucidocynodon riograndensis* (CAPPA/UFSM 0029) from the Late Triassic of Southern Brazil, in left lateral view. **A**. photo, **B**. tridimensional model, and **C**. schematic drawing. **Abbreviations: An**, angular; **apd**, angular process of the dentary; **D**, dentary; **dpf**, dorsal opening of the paracanine fossa; **I1–4**, upper incisors; **iof**, infraorbital foramen; **Ip**, interparietal; **J**, jugal; **L**, lacrimal; **lc**, left lower canine; **lC**, left upper canine; **Mx**, maxilla; **mf**, mental foramen; **msf**, masseteric fossa; **Na**, nasal; **P**, parietal; **Pm**, premaxilla; **Po**, postorbital; **Prf**, prefrontal; **PC1**, upper postcanine; **Q-Qj?**, quadrate-quadratojugal?; **Sa**, surangular; **Sq**, squamosal.

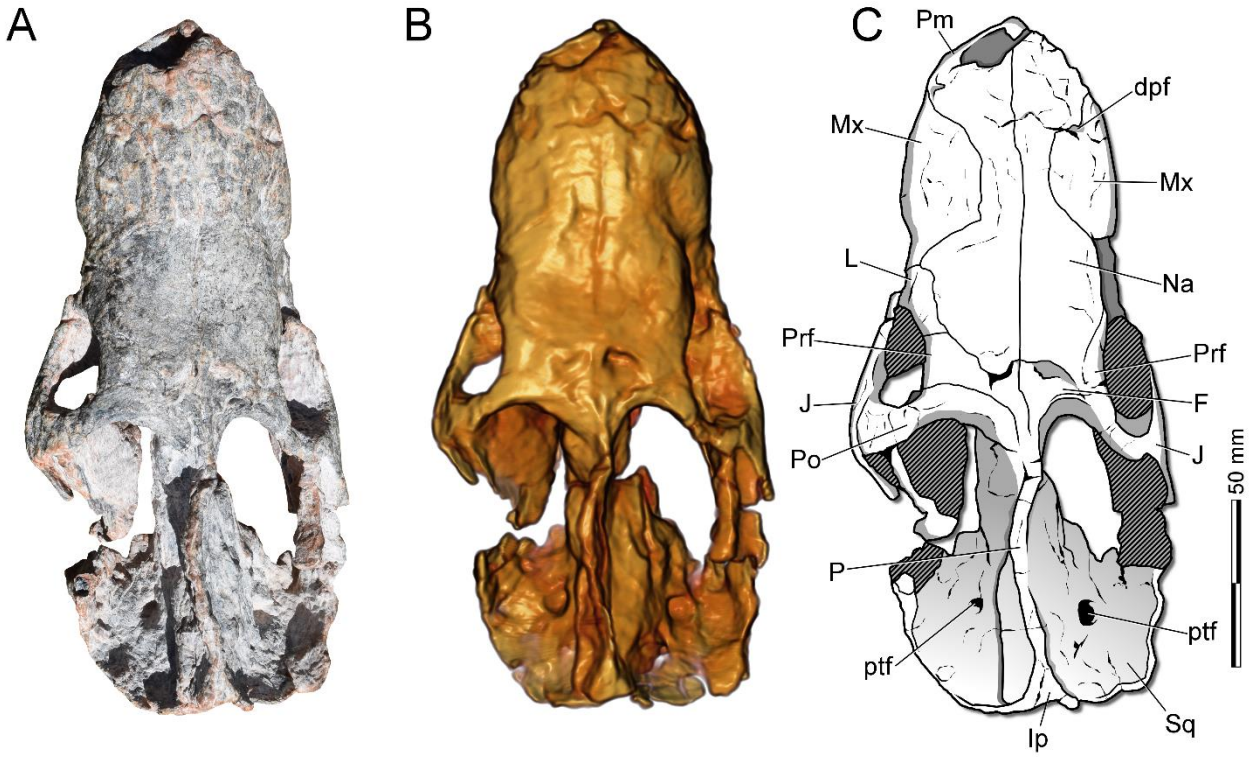

FIGURE 4. Skull and mandible of *Trucidocynodon riograndensis* (CAPPA/UFSM 0029) from the Late Triassic of Southern Brazil, in dorsal view. **A**. photo, **B**. tridimensional model, and **C**. schematic drawing. **Abbreviations: dpf**, dorsal opening of the paracanine fossa; **F**, frontal **Ip**, interparietal; **J**, jugal; **L**, lacrimal; **Mx,** maxilla; **Na**, nasal; **P**, parietal; **Pm**, premaxilla; **Po**, postorbital; **Prf**, prefrontal; **ptf**, post-temporal foramen; **Sq**, squamosal.

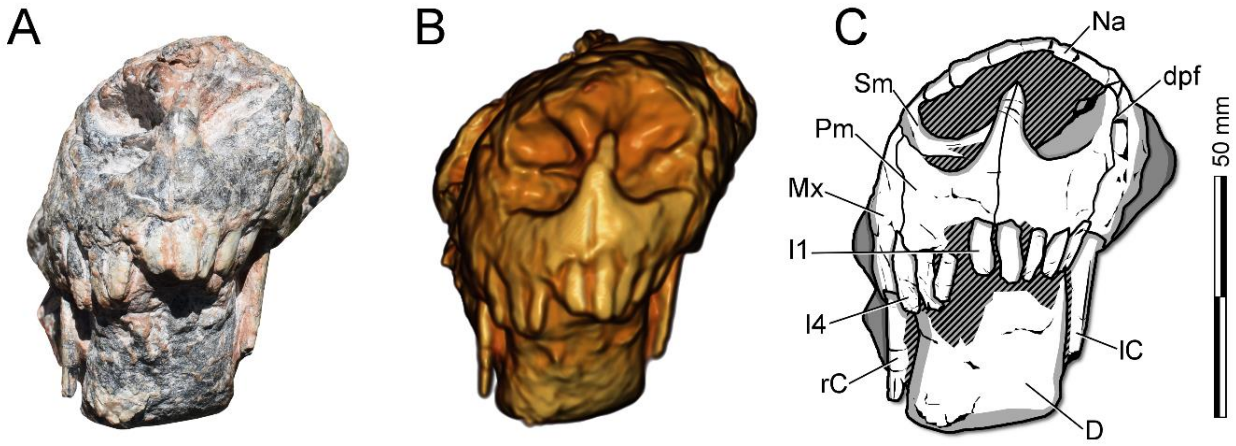

FIGURE 5. Skull and mandible of *Trucidocynodon riograndensis* (CAPPA/UFSM 0029) from the Late Triassic of Southern Brazil, in anterior view. **A**. photo, **B**. tridimensional model, and **C**. schematic drawing. **Abbreviations: D**, dentary; **dpf**, dorsal opening of the paracanine fossa; **I1–4**, upper incisors; **lC**, left upper canine; **Mx**, maxilla; **Na**, nasal; **Pm**, premaxilla; **rC**, right upper canine; **Sm**, septomaxilla.

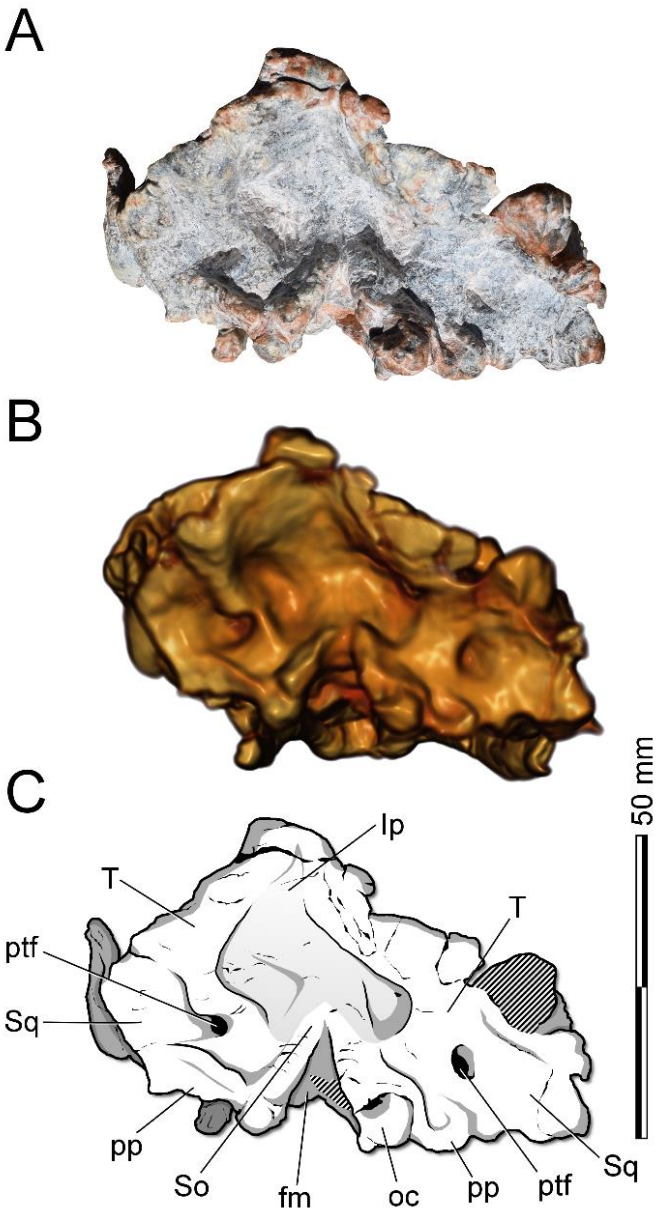

FIGURE 6. Skull and mandible of *Trucidocynodon riograndensis* (CAPPA/UFSM 0029) from the Late Triassic of Southern Brazil, in occipital view. **A**. photo, **B**. tridimensional model, and **C**. schematic drawing. **Abbreviations: fm**, foramen magnum; **Ip**, interparietal; **oc**, occipital condyle; **pp**, paroccipital process of the opisthotic; **ptf**, post-temporal foramen; **So**, supraoccipital; **Sq**, squamosal; **T**, tabular.

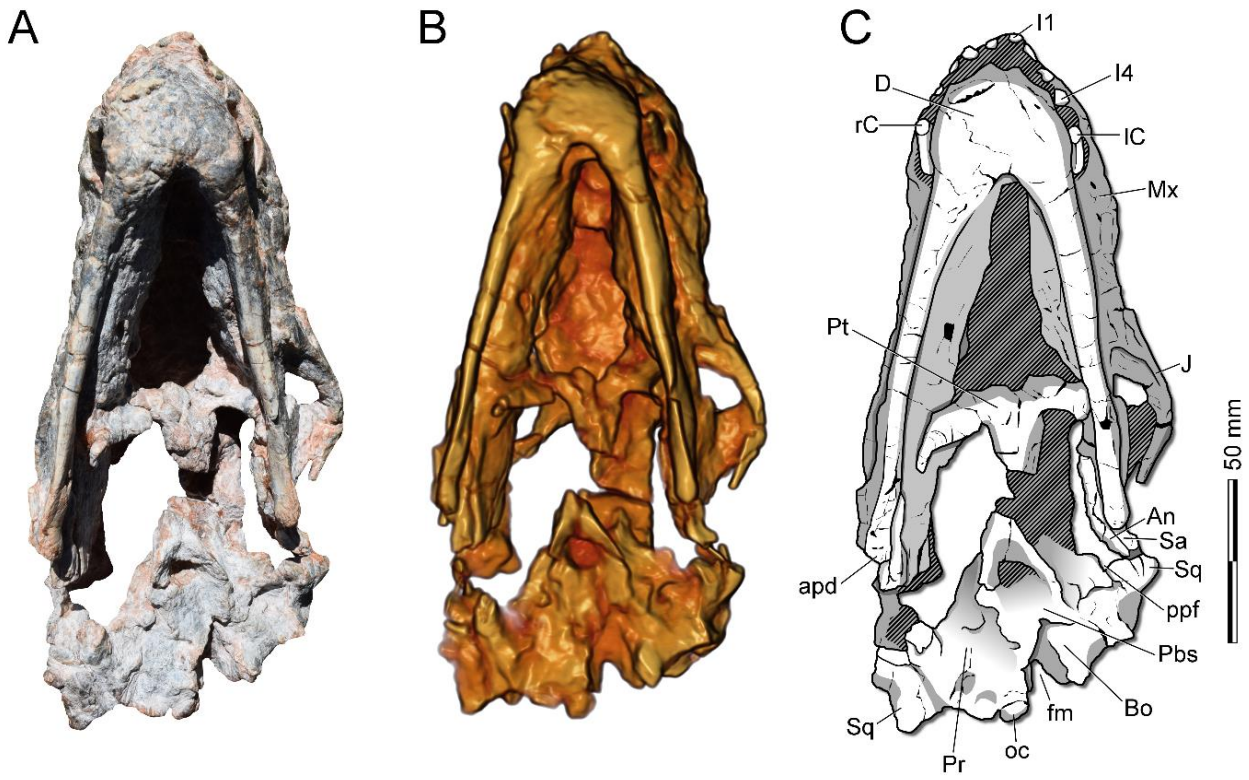

FIGURE 7. Skull and mandible of *Trucidocynodon riograndensis* (CAPPA/UFSM 0029) from the Late Triassic of Southern Brazil, in ventral view. **A**. photo, **B**. tridimensional model, and **C**. schematic drawing. **Abbreviations: An**, angular; **apd**, angular process of the dentary; **Bo**, basioccipital; **D**, dentary; **fm**, foramen magnum; **I1–4**, upper incisors; **lC**, left upper canine; **J**, jugal; **Mx**, maxilla; **oc**, occipital condyle; **Pbs**, parabasisphenoid; **Pr**, prootic; **Pt**, pterygoid; **ppf**, pterygoparoccipital foramen; **rC**, right upper canine; **Sa**, surangular; **Sq**, squamosal.

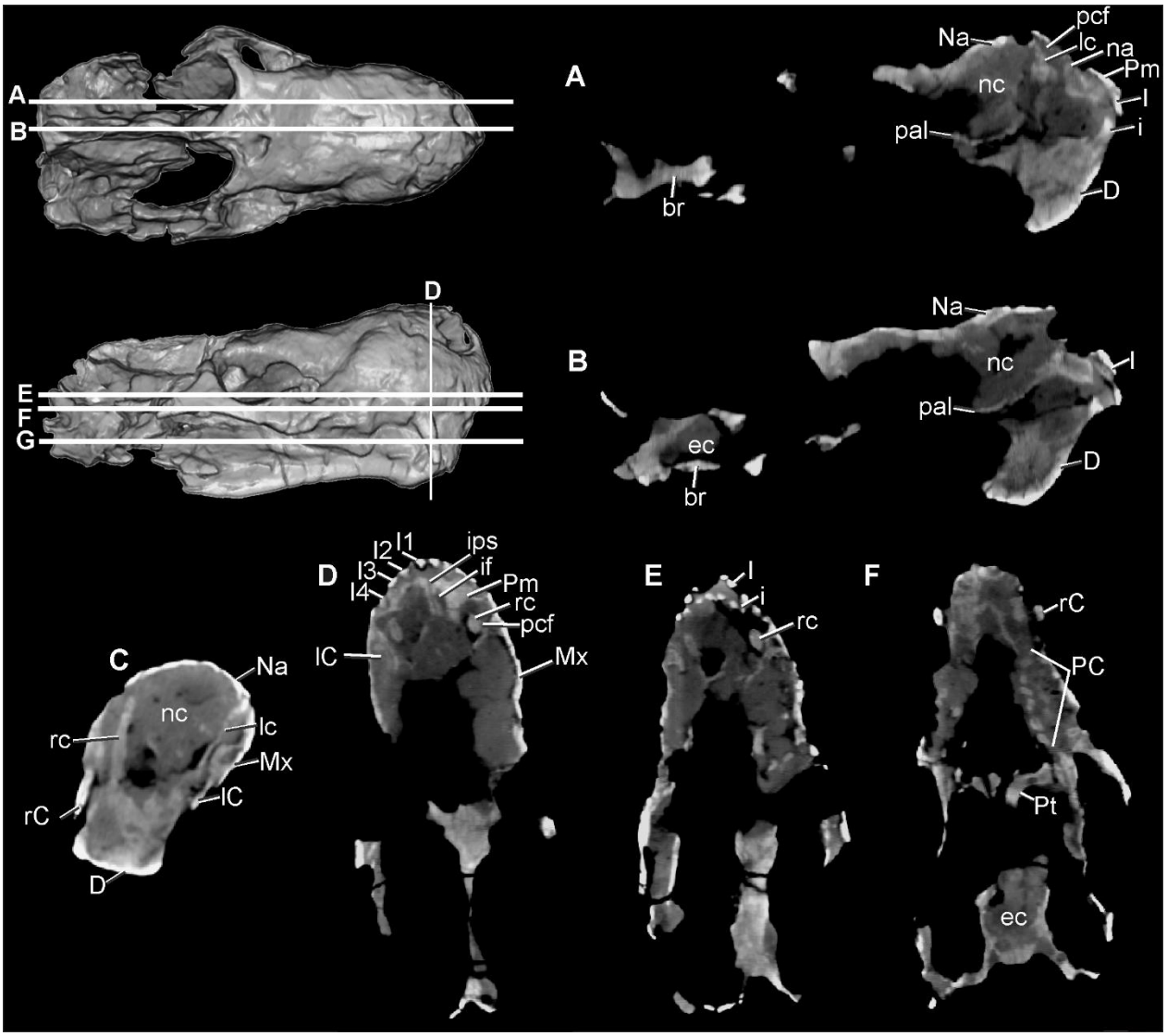

FIGURE 8. Slices of the skull and mandible of *Trucidocynodon riograndensis* (CAPPA/UFSM 0029) in sagittal (**A-B**), coronal (**C**), and horizontal (**D-F**) planes. **Abbreviations: br**, basicranial region; **D**, dentary; **ec,** encephalic cavity; **i**, lower incisors; **I**, upper incisors; **if**, incisive foramen; **ips**, interpremaxillary suture; **lc**, left lower canine; **lC**, left upper canine; **Mx**, maxilla; **Na**, nasal; **na**, narial opening; **nc**, nasal cavity; **pal**, palatal region; **PC**, upper postcanines; **pcf**, paracanine fossa; **Pm**, premaxilla; **Pt**, pterygoid; **rc**, right lower canine; **rC**, right upper canine.

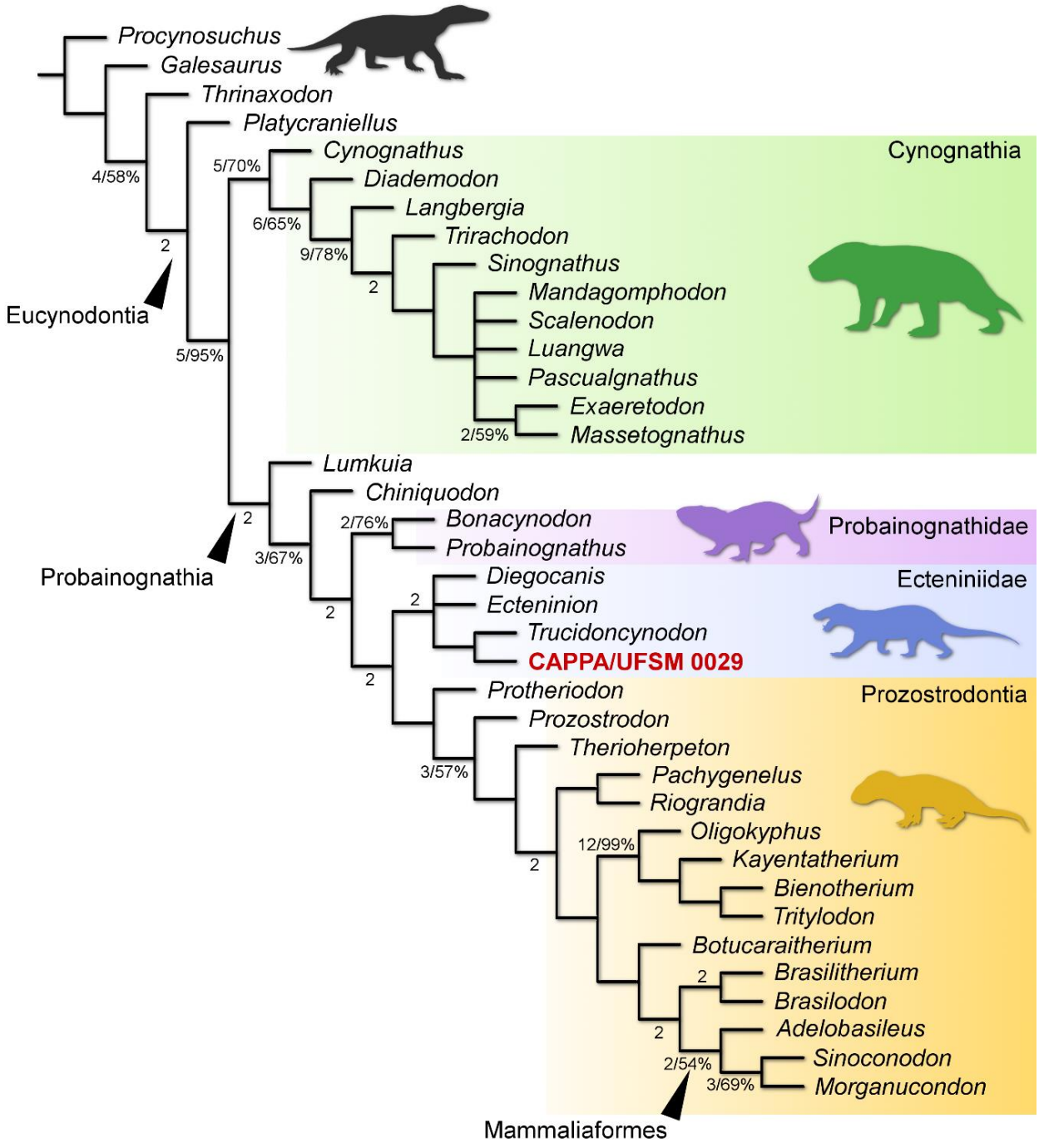

FIGURE 9. Strict consensus cladogram depicting the phylogenetic position of CAPPA/UFSM 0029. Numbers below nodes represent Bremer support values (left) higher than 1 and Bootstrap values (right) higher than 50%.

Supporting information for:

Skull anatomy and a phylogenetic assessment of a large Ecteniniidae (Eucynodontia: Probainognathia) from the Upper Triassic of Southern Brazil

Character list (modified from Liu & Olsen 2010; Martínez et al. 2013; Martinelli et al. 2016)

1. Premaxillary extranasal process: absent or with very little exposure (0); large but not contacting nasal (1); contacting nasal (2).

2. Septomaxilla facial process: long, extending far beyondposterior border of external naris (0); short, almost limited in external naris (1).

3. Muzzle anteroposterior length relative to anteroposterior length of the temporal region (measured from the anteriormost level of the posterior border of postorbital bar): less than 0.95 (0); greater than 0.95 and smaller than 1.05 (1); greater than 1.05 (2); without postorbital bar (3).

4. Position of paracanine fossa in relation to upper canine: anteromedial (0); medial or posteromedial (1); anterior (2); paracanine fossa absent (3).

5. Premaxilla: does not form (0) or does form (1) posterior border of incisive foramen.

6. Maxillary platform lateral to tooth row: absent (0); present (1).

7. Maxilla: excluded from (0) or participates in (1) border of subtemporal fenestra.

8. Profile of skull roof (relationship of sagittal crest with part of skull roof just anterior to it): nearly flat (0); remarkably concave (1); convex (2).

9. Parietal foramen: present (0); absent (1).

10. Interparietal (postparietal) in adult: separate bone (0); absent or fused with other bones (1).

11. Lateral expansion of braincase in parietal region: absent (0); moderate (1); well developed (2).

12. Sagittal crest: does not (0) or does (1) extend posteriorly to reach or closely approach the posteriormost part of the lambdoidal crest.

13. Prefrontal: present (0); absent (1).

14. Postorbital: present and forms postorbital bar (0); present but does not form postorbital bar (1); absent (2).

15. Palatine: does not meet frontal (0); meets frontal but neither element contributes significantly to medial orbit wall (1); meets frontal and both elements contribute significantly to medial orbit wall (2).

16. Sphenopalatine foramen: absent (0); present (1).

17. Dorsoventral height of zygomatic arch as a proportion of skull length: moderately deep (10~18%) (0); very deep (>18%) (1); slender (<10%) (2).

18. Anteroventral corner of zygomatic arch: lies at same level as (0) or lies significantly higher than (1) postcanine line.

19. Infraorbital process: absent (0); suborbital angulation between maxilla and jugal (1); descending process of jugal (2).

20. Maximum dorsal extent of zygomatic arch: below middle of orbit (0); above middle of orbit but below upper border (1); above upper border of orbit (2).

21. Maximum posterior extent of jugal along zygomatic arch: near quadratojugal notch of squamosal (0); near squamosal glenoid (1); receding from glenoid (2).

22. Posteroventral process of jugal: low, forming less than half the height of the zygomatic arch (0); high, forming more than half the height of the zygomatic arch.

23. Width of temporal fossa: greatest near middle (0); constant or nearly constant along its length (1); strongly increasing toward the posterior end (2).

24. Squamosal groove for external auditory meatus: an incipient depression (0); deep (1).

25. Posterior extension of squamosal, dorsal to squamosal sulcus in zygomatic arch: incipient (0); well developed (1).

26. Notch separating lambdoidal crest from zygomatic arch: shallow (0); deep, V-shaped (1).

27. Palatine: excluded from subtemporal border of orbit (0); participates in subtemporal border by displacing pterygoid posteriorly (1).

28. Vomer exposure in incisive foramen (at anterior ends of maxillae on palate): present (0); absent (1).

29. Vomer: with (0) or without (1) vertical septum extending posteriorly beyond level of secondary palate.

30. Ectopterygoid: present, but does not contact maxilla (0); present and contacts maxilla (1); absent (2).

31. Interpterygoid vacuity between pterygoid flanges: present (0); absent (1) in adults.

32. Secondary palatal plate on maxilla: does not extend to midline (0); extends to midline (1).

33. Secondary palatal plate on palatine: does not extend to midline (0); extends to midline (1).

34. Osseous second ary palate: terminates well anterior to last upper postcanine tooth (0); terminates near or well posterior to last upper postcanine tooth (1).

35. Osseous secondary palate: terminates anterior to (0), at approximately the level of (1), or posterior to (2) anterior border of orbit.

36. Anteroposterior extent of osseous secondary palate: 45% of skull length or less (0); more than 45% of skull length (1).

37. Length of palatine relative to maxilla in secondary palate: shorter (0); about equal (1); longer (2).

38. Middle of pterygoid: smooth (0); bears a boss (1); bears a distinct median crest (2).

39. Nasopharyngeal roof posterior to transverse process of pterygoid: narrow, deep, forms a ventral keel (0); flat, minimum width greater than half width of transverse process of pterygoid (1).

40. Quadrate ramus of pterygoid: present (0); absent (1).

41. Quadrate articulation with quadrate ramus of epipterygoid: absent (0); present (1).

42. Frontal-epipterygoid contact: present (0), absent (1).

43. Epipterygoid ascending process at level of trigeminal foramen: greatly expanded (0); moderately expanded (1).

44. Anterior part of basisphenoid: narrow (0); wide, and width greater than half width of transverse process of pterygoid (1).

45. Parasphenoid ala (basisphenoid wing): at same level as basicranium (0); ventrally expanded below basicranium (1).

46. Parasphenoid ala: long, bordering fenestra vestibule (0); slightly shorter and excluded from fenestra vestibuli, but overlapping entire prootic pars cochlearis (a part of the petrosal) (1); much shorter and overlapping prootic pars cochlearis (2); basisphenoid does not overlap prootic pars cochlearis (3).

47. Extent of basioccipital overlap on pars cochlearis: covers entire pars cochlearis (0); covers medial side of promontorium (1); no overlapping (2).

48. Internal carotid foramina in basisphenoid: present (0); absent (1).

49. Prootic and opisthotic: separate (0); fused at early ontogenetic stage to form petrosal (=periotic) (1).

50. Promontorium: absent (0); present (1).

51. Internal auditory meatus: open (0); walled (1).

52. Space for trigeminal ganglion (semilunar ganglion): open ventrally (0); partly floored by prootic (1); completely floored by prootic (2).

53. Lateral trough floor anterior to tympanic aperture of prootic canal and/or primary facial foramen: absent (0); present (1).

54. Vascular foramen in posterior part of lateral flange (Foramen “X” of Rougier et al. 1992: 205): absent (0); present (1).

55. Foramen and passage of prootic sinus in lateral trough: absent (0); present (1).

56. Route of venous drainage from back of cavum epiptericum: only vascular groove on lateral flange (0); absent (1); vascular canal on lateral flange (foramina on lateral surface) (2).

57. Maxillary and mandibular branches (V2+3) of trigeminal nerve exit: via single foramen between prootic and epipterygoid (0); via two foramina between prootic and epipterygoid (1); via separate foramina, some enclosed by anterior lamina of prootic (petrosal) (2).

58. Pterygoparoccipital foramen: squamosal does not contribute to enclosure of foramen (0); squamosal contributes to enclosure of foramen (1); open as a notch (2).

59. Lateral flange of prootic: lacks vertical component (0); includes vertical component, so that flange is Lshaped and forms vertical wall adjacent to pterygoparoccipital foramen.

60. Anterior part of paroccipital process: lateral aspect covered by squamosal (0); lateral aspect exposed due to dorsal withdrawal of squamosal (1).

61. Hyoid (stapedial) muscle fossa on paroccipital process: absent (0); present (1).

62. Paroccipital process: undifferentiated (0); differentiated into a posterior process and a bulbous anterior process (1); differentiated into mastoid and quadrate processes (2).

63. Fenestra rotunda and jugular foramen: confluent (0); completely and widely separated (1).

64. Paroccipital process: does not contact quadrate (0); contacts quadrate (1).

65. Paroccipital process in base of posttemporal fossa: absent (0); present (1).

66. Tabular: present (0); absent (1).

67. Relationship of hypoglossal foramen (condylar foramen) with jugular foramen: confluent or sharing a depression (0); at least one foramen completely separated from jugular foramen (1).

68. Shape of occipital condyles (in lateral view): bulbous (0); ovoid to cylindrical (1).

69. Rotation of dorsal plate relative to trochlear axis of quadrate: small (less than 10 degrees) (0); about 45 degrees (1); around 90 degrees (2); parallel to trochlear axis (3).

70. Contact facet on posterior side of dorsal plate of quadrate: flat or convex (0); concave (1).

71. Trochlear condyles of quadrate: lateral condyle larger than medial condyle (0); medial condyle at least as large as lateral condyle (1).

72. Shape of trochlea of quadrate: cylindrical (0); troughshaped (1).

73. Lateral margin of dorsal plate of quadrate: straight (0); flaring posteriorly (1); flaring and rotated posteromedially (2).

74. Medial margin of dorsal plate of quadrate: straight (0); flaring anteriorly (1); flaring and rotated anterolaterally (2).

75. Dorsal margin of dorsal plate of quadrate: with a pointed dorsal process (“dorsal angle”) (0); rounded (1).

76. Lateral notch and neck of quadrate (separating lateral margin of contact facet from trochlea): lateral notch absent or poorly developed (0); lateral notch developed, separating lateral margin of contact facet fromlateral end of trochlea (1); lateral notch broader, separation of lateral margin of contact facet from trochlea wider, lateral margin shifted medially (2); neck developed, displacing contact facet away from trochlea (3).

77. Articulation of quadrate with squamosal: via an anteriorly open and concave recess in the squamosal (0); anteriorly open squamosal recess is absent (1); quadrate having little or no contact with the squamosal (2).

78. Articulation of quadrate with stapes: via broad recess on medial margin and medial end of trochlea (0); stapedial contact restricted to medial end of trochlea (1); via projection from medial margin of dorsal plate (2); via medial vertical ridge on neck of quadrate (3); via projection from neck of quadrate (4).

79. Craniomandibular articulation: quadrate/articular (0); primarily quadrate/articular, secondarily surangular/ squamosal (1); incipient dentary/squamosal (2); primarily dentary/squamosal (3).

80. Craniomandibular articulation: around dorsoventral level of postcanine line (0), much lower than postcanine line (1); much higher than postcanine line (2).

81. Squamosal articular surface for mandible: absent (0); formed by small and medially or anteromedially facing facet (1); wide glenoid cavity directed approximately ventrally (2).

82. Dentary symphysis: unfused (0); fused (1).

83. Lateral crest of dentary: absent (0); incipient (1); moderately developed (2); strongly projecting (3).

84. Angle of dentary: close to anteroposterior position of postorbital bar (0); close to jaw joint (1).

85. Anteroposterior position of dorsal contact between dentary–surangular, relative to postorbital bar and jaw joint: around midway between these landmarks (0); closer to jaw joint (1).

86. Inner side of coronoid process (including coronoid bone): relatively thin (0); mediolaterally thick (1).

87. Splenial: large and deep, reaches ventral border of dentary (0); thin splint covering dentary groove (1).

88. Postdentary bones: large, including tall surangular (0); angular, surangular, and prearticular medium in height and lying in dentary groove (1); single gracile rod in postdentary trough (2).

89. Posterior extent of reflected lamina of angular: greaterthan 1/2 distance from angle of dentary to jaw joint (0); less than l/2 this distance (1).

90. Reflected lamina of angular in lateral view: spoonshaped plate bearing slight depressions (0); hook-like lamina (1); thin process (2)

91. Mandibular movement during occlusion inferred from wear facets: orthal movement during power stroke (0); posteriorly directed power stroke (1); moderate rotation along longitudinal axis during power stroke (2).

92. Postcanine occlusion: no consistent pattern of contact between upper and lower tooth rows (0); bilateral, interdigitating occlusion between multiple cusps (1); precise unilateral occlusion (2).

93. Wear facets on postcanines: absent (0); simple longitudinal facet present on crown (1); main cusp bears two distinct facets (2); multiple cusps each bear one or two transverse and crescentic facets (3).

94. Number of upper incisors: five or more (0); four (1); three or less (2).

95. Number of lower incisors: four or more (0); three (1); two or less (2).

96. Incisors: all of similar size (0); some incisor large (1).

97. Incisor cutting margins: smoothly ridged (0); serrated (1); denticulated (2).

98. Distinct diastema between upper incisor and canine: present (0); absent (1).

99. Upper canine: large (0); small (height <10% of skull length) (1); absent (2).

100. Lower canine: large (0); small (1); absent (2).

101. Canine serrations: absent (0); present (1).

102. Upper postcanine: sectorial, lacking cingulum or with incipient lingual cingulum (0); sectorial, with well-developed lingual cingulum (1); buccolingually expanded (2).

103. Single-cusped tooth as anteriormost postcanine: present in juveniles and adults (0); present only in juveniles (1); absent (2).

104. Gomphodont tooth as posteriormost postcanine: absent (0); absent in juveniles but present in adults (1); present in both juveniles and adult (2).

105. Main cusps of posterior postcanine teeth: not strongly curved (0); strongly curved (1).

106. Upper postcanine roots: single (0); constricted root, with incipient longitudinal groove (1); divided into two longitudinal aligned roots (2); multiple roots (more than two) (3).

107. Lower postcanine roots: single (0); constricted root, with incipient longitudinal groove (1); divided (2).

108. Buccal (external) cingulum on sectorial upper postcanines: absent (0); present (1).

109. Transverse crest in upper postcanines: absent (0); present with two cusps (1); present with three or more cusps (2).

110. Position of transverse row of upper postcanines: midcrown (almost to posterior margin) (0); on anterior half of crown (1); at posterior margin of crown (no posterior cingulum) (2).

111. Central cusp of transverse row of upper postcanines: absent (0); midway between buccal and lingual cusps (1); closer to lingual cusp (2).

112. Alignment of main cusps of upper postcanines: single longitudinal row (0); multiple cusps in multiple rows (1).

113. Contacts between adjacent lower postcanines: simple, with no interlocking (0); distal cuspule ofanterior molar fits into embayment between cusps of succeeding molar (1).

114. Number of cusps in transverse row of lower postcanines: two (0); three or more (1).

115. Lingual cingulum on lower postcanine: present (0); vestigial or absent (1).

116. Lower posterior basin: absent (0); present (1).

117. Axis of posterior part of maxillary tooth row: directed lateral to subtemporal fossa (0); directed toward center of fossa (1); directed toward medial rim of fossa and diverged curved (2); directed toward medial rim of fossa and straight (3).

118. Posterior end of upper tooth row: below orbit and anterior to subtemporal fenestra (0); anterior to orbit (1); posterior to anterior border of subtemporal fenestra (2).

119. Postcanine replacement pattern: alternating (0); delayed (1); sequential addition of postcanines, no replacement (2).

120. Vertebral centra: amphicoelous (0); platycoelous (1).

121. Axial centrum: cylindrical (0); depressed (1). [R98] 122. Dens: absent or vestigial (0); strongly developed (1).

123. Posterior thoracic vertebrae (or mid-dorsal vertebrae): neural spines nearly vertical or slightly inclined (0) or strongly inclined (1).

124. Anapophysis: absent (0); present (1).

125. Expanded costal plates on dorsal ribs: absent (0); present (1).

126. The ridge on lumbar costal plates overlapping preceding rib: absent (0); present (1).

127. Acromion process: absent (0); weakly to moderately developed (1); strongly developed and close to level of glenoid (2).

128. Scapular constriction below acromion: absent (0); present (1).

129. Scapular elongation between acromion and glenoid: absent (0); present (1).

130. Procoracoid contribution to glenoid fossa: present (0); barely present or absent (1).

131. Procoracoid contact with scapula: longer than coracoid contact (0); equal to or shorter than coracoid contact (1).

132. Ectepicondylar foramen in humerus: present (0); absent (1).

133. Olecranon process of ulna: unossified or poorly ossified (0); well ossified (1).

134. Number of phalanges present in manual digit III: four (0); three (1).

135. Number of phalanges present in manual digit IV: four (0); three (1).

136. Dorsal profile of ilium in lateral view: stronglyconvex (0); straight to concave (1).

137. Length of anterior process of ilium anterior to acetabulum: less than 1.5 times diameter of acetabulum (0); greater than 1.5 times diameter of acetabulum (1).

138. Lateral surface of iliac blade: concave or nearly flat (0); convex (1); divided by longitudinal ridge into dorsal and ventral portions (1).

139. Posterior iliac spine: robust and extends beyond acetabulum (0); small nub that lies entirely anterior to acetabulum (1).

140. Cotyloid (acetabular) notch: lies between ischial and iliac parts of acetabulum, but mainly on ilium (0); lies entirely on ischium, between acetabular facet and pubic process (1).

141. Diameter of obturator foramen: less than or equal to that of acetabulum (0): greater than that of acetabulum (1).

142. Head of femur: rounded and predominantly in plane of shaft (0); subspherical and inflected dorsally (1).

143. Greater trochanter of femur: continuous with femoral head (0); separated from femoral head by distinct notch (1).

144. Lesser trochanter: on ventromedial surface of femoral shaft (0); on medial surface of femoral shaft (1).

145. Lesser trochanter: far distally from femoral head (0); near level of femoral head (1).

146. Profile of the anterior region of muzzle in lateral view: sub-rectangular (0); subtrapezoidal, anteriorly cuneiform-shaped (1).

147. Temporal region length relative to sagittal crest length: longer (0); almost equal (1).

148. Orbit height relative to snout height (measured al the middle of the external naris): greater than 1 (0); less than or equal to 1 (1).

Character-taxon matrix used in the phylogenetic analysis

Procynosuchus
00200001000000000000000000000000000000000000000000000000000001[01]0000000000
00000000000010000000001000100000000??00?000000000000?0000000000000000002000

Galesaurus
01200000000000000010000010000110000000000000000000000000000000000000000000000
10000100000000001100100000010000??00?1000000001100????00??0??0000000011

Thrinaxodon
01200000000000000000000000000111000000000000000000000000000000000000010010
10000100000110001100000010000000??00?1000000001100?000000000?0000?010

Platycraniellus
01000000000000000011000000000101100000000??00000000?000000000000000000101??101
000?1010?0??0001?0?100000000000??0??0?000??????????????????????????????010

Cynognathus
00200000000000001021002110000011100001011100010100?000000000000010000011100101
10112010111200011010001000100000??00?100100000011100000011000000000011

Diademodon
[01]000000000000000102201211100011110000011100010100000000[01]0000000000000001
00101111120101112113110100012001000100100?000100001111000000110000000000010

Trirachodon
11?00100[01]000000011210111110100111010020111000101000000021000000000001101110
20110111010111211311010001211100020110100101???01111000000????00000000??0

Sinognathus
10?0?100100000??11010011110?1?1?1010?001100001010000?????00000?000?011011102011
01110101 1??113120000002?0?00?201100?0201??????????????????????????????

Langbergia
00?000000000000001210111110100111010000110000101?0?000?21??0000000001?0?11????1
01110101112113110100012001000201101001015?????1?????????????????????????0

Pascualgnathus
1000?100100000001122012111011?1110100001??000101?0???0?2?00000???0?0??????????[0
1]0?1201011??113210000002[12][12]000?110100?12010???1101??0000??1000000000010

Luangwa
???0?1000?000001012100111 1????1110?00001???00101000000?2??00000???0???????????101
1201011??113110100012[12][12]000?202100?12010???110110000???110000000001?

Massetognathus
012111001000000011010111110112111020000100000101000000121100000000000110111020
11011[12]01011??113110211102110 00?222100?120100000101101000??1100000000010

Exaeretodon
002111101000001111210121110112111 01[01]00010?000101000100021100000000000?101????
011011211011??113210010102[12][12]000?120100?122100000001101001111100000000011

Scalenodon
???0?1?0000000??1101012111?????1101?0??1??00010100?00002110000 00?000??0?????0?[01
]0?12??011??113110100012[12][12]000?202100?1201??????????????????????????????

Mandagomphodon
???0010?????001?11?????111011211101?0?0?0??00????????????1?000?0?????1??1?0?0?[01]?
?1???011??113220001002[12][12]000?222100?1201??????????????????????????????

Chiniquodon
110010101000001010110000001011[12]111121000110000101000000010000000000000?1?01???
11101120101112000110000000001000 0??00?100000??000011010001110000?0000010

Lumkuia

??0000101000000?00000000010?120110100101010001001O?0000001000000000000000100001
10112010001200011000000000100O0??00?10000?????001?????????????0?????010

Probainognathus
0100100210000010010110000101121111100001110001000000001100000000000011001102 1
1102100101112000110000000000000??00?10110000?000110???0??11000?0000010

Bonacynodon
?????0?21??000??01011000?10??211111000?????0?????0???????????0??000???????????0?00
01?1112?001?0000?100000000??00??0110?????????????????????????????

Therioherpeton
??3??0121?11122?2100??0????????1111???
?????000????????0?0?1100??00??00000??1?00?????????111111001l0??

Protheriodon
?????0??????????20001?0???????011110???0?1?0?
??11?????100001?00?000000??00??010?????????????????????????????

Riograndia
203310121111122121001000001112011121201100010200O?0000102000010001121102?13??
?000301111??00121100110010011OO??00?10100?????????????????????????010

Pachygenelus
2033101211111221210010000001120111212011000102000010000102000010l??12110221313
2020301111120012210010001000010??00?002001???0001111101??1111111111?10

Prozostrodon
213010?2????1221?1?????????112?1111?1???030
1111??00100000001110011OO??00?001000???000?????0???1111110000?10

Botucaraitherium
?????0??0???11
????01??????001?001110??01?00??0??????????????????????????????

Brasilodon
[01]030?012112112212000100O?00?120111111211000102100l?0?112220?0011101121102213
1320?0301111??00111000010110011l0??01?001[01][01]??????0111??11????????????010

Brasilitherium
00?0?012112112212000100000O?120111110211000102101l?01112220???11?0112110221313
2010301111??00101000010110011l0??01?001[01]1????????????11????????1111???

Tritylodon
103?1111110112211102001111011211102122110000110110110102121111011010311022031 2
0200311111??1132210?22?222?32?2?1100?03221??????210??????1?????1111?10

Oligokyphus
[12]?3?1111?10112???102010110?1?2?1??21????????110?1011010?2?1111011000310022031
20200311111??1132110?22?222?32?2?1100?0322111100?2101111??1121111111?1?

Bienotherium
103?1111110122111?201?11101121110212211000011011011O?02?01111?110?031??22131?0
200311111??1132110?22?222?32?2?1100?03221??????210??11?????111111101?

Kayentatherium
103?11111?01122111020111111112011021221100001101101101021211 1?110?03110221312
020031111112113211O?22?222?32?2?1100?0322?11100021011?1111121??1111010

Adelobasileus
??3????01121?2??????????????????0??????2110001021011?2111221000010111O?????????????
??01?

Sinoconodon
0032?0101121122120001000?01?12111121021100110310 11?2111222101110101O????????0?3
020301112??2001000001001002210??00?10101??????????????????????????010

Morganucodon
0?32?0101121122120002?000011111111210211001103201112111222011211111121102213 24
3020301112122221000001011002210??01?00101111110011111111??1121111111010

Ecteninion
0010100010010 01?2000001001011?1110000201110001000001000101000000000011001102 11
1011011011??000110000010001000O??00?100000????0?21?101???1101?1????000

Diegocanis
00?010??????001??00???????011??1100?0??
?????0?01???00??000?0?00??00?1?000??????????????????????????0?0

Trucidocynodon
1010000010010 01?2000?01001011?1110000??1110001?10001000?020000000010??????????0
0010110?1??000110100010001000O??00?1000?0?1??0?210?011??1101?11?00000

CAPPAUFSM0029
1010?0001?0100??2000?010?1????1????????11??00???00???????2??00?0?0?0????????1??0?10
11011??00?1?1?000??0010?00??00???00??????????????????????????000

4 CONCLUSÃO

Apesar das inúmeras descobertas fósseis para os estratos do Triássico Médio e Superior na América do Sul, sobretudo no Brasil e na Argentina, o registro fóssil de Ecteniniidae ainda é escasso. Nesta presente dissertação de Mestrado, relatamos um crânio e mandíbula quase completos de um novo e grande espécime de *Trucidocynodon riograndensis* Oliveira et al., 2010. Este novo registro de ecteniniídeo aumenta a representatividade do grupo para o Triássico Superior da Supersequência Santa Maria, Sequência Candelária – Carniano, no sul do Brasil.

As análises filogenéticas suportaram CAPPA/UFSM 0029 em uma relação de grupo-irmão com *T. riograndensis* (UFRGS PV-1051-T), ambos em uma tricotomia com *Ecteninion lunensis* e *Diegocanis elegans*, aninhados dentro de Ecteniniidae, com este clado em posição mais derivada que Probainognathidae (*sensu* ROMER, 1973) (*Probainognathus jenseni* e *Bonacynodon schultzi*) e ainda como grupo-irmão de Prozostrodontia (*sensu* LIU & OLSEN, 2010).

CAPPA/UFSM 0029 compartilha com o holótipo UFRGS PV-1051-T uma combinação única de caracteres, o que permitiu atribuí-lo a *T. riograndensis*: (i) processo extranasal do pré-maxilar grande, mas não contatando o nasal; (ii) forame pterigoparoccipital aberto anteriormente; (iii) abertura posterior do forame pós-temporal limitada pelo tabular e esquamosal; e (iv) abertura dorsal externa da fossa paracanina. O novo espécime é aproximadamente 17% maior do que o holótipo UFRGS PV-1051-T, estudado inicialmente por Oliveira et al. (2010). Os espécimes *E. lunensis* e a porção cranial preservada de *D. elegans* são aproximadamente 56,25% e 58,85% menores do que CAPPA/UFSM 0029, respectivamente. Dessa forma, o novo espécime compreende o maior ecteniniídeo coletado até o presente momento.

CAPPA/UFSM 0029, juntamente com o holótipo de *T. riograndensis*, *E. lunensis* e *D. elegans*, fornece evidências adicionais de que os cinodontes probainognátios carnívoros desempenharam um papel significativo nos ecossistemas do Triássico Superior, além de representar uma radiação endêmica no sudoeste do Gondwana. CAPPA/UFSM 0029 representa um dos maior terápsido carnívoro até o momento para o Triássico Superior e contribui para o conhecimento da variação do tamanho corporal dos ecteniniídeos.

REFERÊNCIAS BIBLIOGRÁFICAS

ABDALA, F. Redescription of *Platycraniellus elegans* (Therapsida, Cynodontia) from the Lower Triassic of South Africa, and the cladistic relationships of eutheriodonts. **Palaeontology**, v. 50, p, 591-618, 2007.

ABDALA, F.; BARBERENA, M. A.; DORNELLES, J. A new species of the Traversodontid Cynodont *Exaeretodon* from the Santa Maria Formation (Middle/Late Triassic) of southern Brazil. **Journal of Vertebrate Paleontology**, v. 22, p. 313-325, 2002.

ABDALA, F.; NEVELING, J.; WELMAN, J. A new trirachodontid cynodont from the lower levels of the Burgersdorp Formation (Lower Triassic) of the Beaufort Group, South Africa and the cladistic relationships of Gondwanan Gomphodonts. **Zoological Journal of the Linnean Society**, v. 147, p. 383-413, 2006.

ABDALA, F. et al. South American Middle Triassic continental faunas with Amniotes: Biostratigraphy and Correlation. **Palaeontologia Africana**, v. 44, p. 83-87, 2009.

ABDALA, F.; RIBEIRO, A. M. Distribution and diversity patterns of Triassic cynodonts (Therapsida, Cynodontia) in Gondwana. **Palaeogeography, Palaeoclimatology, Palaeoecology**, v. 286, p. 202-217, 2010.

BONAPARTE, J. F. Sobre nuevos Terápsidos Triásicos hallados en el centro de la Provincia de Mendoza, (Therapsida, Dicynodontia y Cynodontia). **Acta Geológica Lilloana**, v. 8, p. 95-100, 1966.

BONAPARTE, J. F. Dos nuevas "faunas" de reptiles triásicos de Argentina. **Gondwana Stratigraphy**, I.U.G.S., Coloquio Mar del Plata 1967, p. 283-302, 1969.

BONAPARTE, J. F. Los tetrápodos del sector superior de la Formación Los Colorados, La Rioja, Argentina (Triásico Superior). **Opera Lilloana**, v. 22, p. 1-183, 1971.

BONAPARTE, J. F.; MARTINELLI, A. G.; SCHULTZ, C. L.; RUBERT, R. The sister group of mammals: small cynodonts from the Late Triassic of southern Brazil**. Revista Brasileira de Paleontologia**, v. 5, p. 5-27, 2003.

BONAPARTE, J. F.; MARTINELLI, A. G.; SCHULTZ, C. L. New information on *Brasilodon* and *Brasilitherium* (Cynodontia, Probainognathia) from the Late Triassic of southern Brazil. **Revista Brasileira de Paleontologia**, v. 8, p. 25-46, 2005.

BONAPARTE, J. F.; MIGALE, L. A. **Protomamíferos y Mamíferos Mesozoicos de América del Sur**. Mercedes, Buenos Aires, Argentina: Museo Municipal de Ciencias Naturales Carlos Ameghino, p. 1-441, 2010.

BONAPARTE, J. F.; SOARES, M. B.; MARTINELLI, A. G. Discoveries in the Late Triassic of Brazil improve knowledge on the origin of mammals. Historia Natural, Fundación Felix de Azara. **Tercera Serie**, v. 2, p. 5-30, 2012.

BOTHA, J.; ABDALA, F.; SMITH, R. The oldest Cynodont: new clues on the origin and early diversification of the Cynodontia. **Zoological Journal of the Linnean Society**, v. 149, p. 477-492, 2007.

CABREIRA, S. F. et al. New stem-sauropodomorph (Dinosauria, Saurischia) from the Triassic of Brazil. **Naturwissenschaften**, v. 98, p. 1035-1040, 2011.

CROMPTON, A. W. Postcanine occlusion in Cynodonts and Tritylodonts. Bulletin of the British Museum (Natural History). **Geology**, v. 21, p. 29-71, 1972.

HOPSON, J. A.; BARGHUSEN, H. An analysis of Therapsid relationships. In: HOTTON, N.; MACLEAN, P. D.; ROTH, J. J.; ROTH, E. C. **The ecology and biology of mammal-like reptiles.** Smithsonian Institution Press, Washington DC, p. 83-106, 1986.

HOPSON, J. A.; KITCHING, J. W. A probainognathian cynodont from South Africa and the Phylogeny of nonmammalian Cynodonts. **Bulletin of the Museum of Comparative Zoology**, v. 156, p. 5-35, 2001.

HORN, B. L. D. et al. A new third-order sequence stratigraphic framework applied to the Triassic of the Paraná Basin, Rio Grande do Sul, Brazil, based on structural, stratigraphic and paleontological data. **Journal of South American Earth Sciences**, v. 55, p. 123-132, 2014.

KAMMERER, C. F. A new taxon of cynodont from the Tropidostoma Assemblage Zone (upper Permian) of South Africa, and the early evolution of Cynodontia. **Palaeontology**, v. 2, p. 387-397, 2016.

KEMP, T. S. **Mammal-like Reptiles and the Origin of Mammals.** Academic Press, London, p. 363, 1982.

LANGER, M. C.; RIBEIRO, A. M.; SCHULTZ, C. L.; FERIGOLO, J. The continental Tetrapod bearing Triassic of south Brazil. **Bulletin of the New Mexico Museum of Natural History and Science**, v. 41, p. 201-218, 2007.

LANGER, M. C.; RAMEZANI, J.; DA ROSA, Á. A. U-Pb age constraints on dinosaur rise from south Brazil. **Gondwana Research.** v. 57, p. 133-140, 2018.

LIPARINI, A. et al. The lower jaw and dentition of the Traversodontid *Exaeretodon riograndensis* Abdala, Barberena, Dornelles, from the Brazilian Triassic (Santa Maria 2 Sequence, Hyperodapedon Assemblage Zone). **Alcheringa**, v. 37, p. 1-23, 2013.

LIU, J.; ABDALA, F. Phylogeny and taxonomy of the Traversodontidae. In Early evolutionary history of the Synapsida. **Springer Netherlands**, p. 255-279, 2014.

LIU, J.; OLSEN, P. E. The phylogenetic relationships of Eucynodontia (Amniota, Synapsida). **Journal of Mammalian Evolution**, v. 17, p. 151-176, 2010.

LUO, Z. -X. Sister-group relationships of mammals and transformations of diagnostic mammalian characters. In: Fraser, N. C.; Sues, H. -D. **In the Shadow of the Dinosaurs - Early Mesozoic Tetrapods.** Cambridge University Press, Cambridge, p. 98-128, 1994.

MARTINELLI, A. G.; ROUGIER, G. W. On *Chaliminia musteloides* Bonaparte (Cynodontia, Tritheledontidae) and the phylogeny of the Ictidosauria. **Journal of Vertebrate** Paleontology, v. 27, p. 442-460, 2007.

MARTINELLI, A. G.; SOARES, M. B. **Evolution of South American cynodonts.** Contrib Mus Argent Cienc Nat "Bernardino Rivadavia", v. 6, p. 183-197, 2016.

MARTINELLI, A. G.; SOARES, M. B.; SCHWANKE, C. Two New Cynodonts (Therapsida) from the Middle-Early Late Triassic of Brazil and Comments on South American Probainognathians. **Plos One**, v. 11(10): DOI: 10.1371, 2016.

MARTINELLI, A. G.; ELTINK, E.; DA-ROSA, A. A. S.; LANGER, M. C. A new cynodont from the Santa Maria Formation, south Brazil, improves late Triassic probainognathian diversity. **Pap Palaeontology**, v. 3, p. 401, 2017.

MARTÍNEZ, R. N.; FORSTER, C. A. The skull of *Probelesodon sanjuanensis*, sp. nov., from the Late Triassic Ischigualasto Formation of Argentina. **Journal of Vertebrate Paleontology**, v. 16, p. 285-291, 1996.

MARTÍNEZ, R. N.; MAY, C. L.; FORSTER, C. A. A new carnivorous cynodonts from the Ischigualasto Formation (Late Triassic, Argentina), with comment on eucynodont phylogeny. **Journal of Vertebrate Paleontology**, v. 16, p. 271-284, 1996.

MARTÍNEZ, R. N.; FERNANDEZ, E.; ALCOBER, O. A. A new nonmammaliaform Eucynodont from the Carnian-Norian Ischigualasto Formation, northwestern Argentina. **Revista Brasilera de Paleontología**, v. 16, p. 61-76, 2013.

MÜLLER, R. T.; LANGER, M. C.; CABREIRA, S. F.; DIAS-DA-SILVA, S. The femoral anatomy of *Pampadromaeus barberenai* based on a new specimen from the Upper Triassic of Brazil. **Historical Biology**, v. 28, p. 656-665, 2016.

MÜLLER, R. T.; MAX, C. L.; PACHECO, C. P.; DIAS-DA-SILVA, S. The role of ontogeny on character polarization in early dinosaurs: a new specimen from the Late Triassic of southern Brazil and its implications. **Historical Biology**, p. 1-12, 2017.

MUSSER, A. M. et al. First australian non-mammalian cynodont: New evidence for the unusual nature of Austrália Cretaceous Vertebrates. **12th Conference on Australasian Vertebrate Evolution, Paleontology and Systematics,** 2009.

OLIVEIRA, T. V.; SCHULTZ, C. L.; SOARES, M. B. O esqueleto pós-craniano de *Exaeretodon riograndensis* et al. (Cynodontia, Traversodontidae), Triássico do Brasil. **Revista Brasileira de Paleontologia**, v. 10, p. 79-94, 2007.

OLIVEIRA, T. V.; SOARES, M. B.; SCHULTZ, C. L. *Trucidocynodon riograndensis* gen. nov. et sp. nov. (Eucynodontia), a new cynodont from the Brazilian Upper Triassic (Santa Maria Formation). **Zootaxa**, v. 2382, p. 1-71, 2010.

OWEN, R. **Palaeontology, or a Systematic Summary of Extinct Animals and Their Geological Relationships**. Adam and Black, Edinburgh, p. 463, 1861.

ROMER, A. S. The Chanares (Argentina) Triassic reptile fauna. XVIII. *Probelesodon minor*, a new species of carnivorous cynodont; family Probainognathidae nov. **Breviora**. v. 401, p. 1-4, 1973.

ROWE, T. Definition, Diagnosis and Origin of Mammalia. **Journal of Vertebrate Paleontology**, v. 8, p. 241-264, 1988.

SOARES, M. B.; SCHULTZ, C. L.; HORN, B. L. D. New information on *Riograndia guaibensis* Bonaparte, Ferigolo, Ribeiro, 2001 (Eucynodontia, Tritheledontidae) from the Late Triassic of southern Brazil: anatomical and biostratigraphic implications. **Anais da Academia Brasileira de Ciências**, v. 83, p. 329-354, 2011.

SOARES, M. B.; MARTINELLI1, A. G; OLIVEIRA, T. V. A new prozostrodontian cynodont (Therapsida) from the Late Triassic Riograndia Assemblage Zone (Santa Maria Supersequence) of Southern Brazil. **Anais da Academia Brasileira de Ciências**, v. 86, p. 1673-1691, 2014.

WATABE, M.; TSUBAMOTO, T.; TSOGTBAATAR, K. A new Tritylodontid Synapsid from Mongolia**. Acta Palaeontologica Polonica**, v. 52, p. 263-274, 2007.